Quantum Chaos and Quantum Ergodicity

A. Bäcker and F. Steiner

Abteilung Theoretische Physik, Universität Ulm, Albert-Einstein-Allee 11, D–89069 Ulm, Germany

Abstract. We report on some of our results which have been achieved within the *DFG Schwerpunktprogramm "Ergodentheorie, Analysis und effiziente Simulation dynamischer Systeme" (1994-2000)*. One main point of our research programme has been the search for universal statistical properties of energy spectra and eigenfunctions of quantum mechanical systems whose classical dynamics is chaotic. The mode-fluctuation distribution $P(W)$ has been proposed as a universal signature of quantum chaos and a conjecture on its limit distribution has been put forward. The conjecture turns out to be mathematically equivalent to a hypothesis on the value distribution of dynamical zeta functions on the critical line and has been successfully tested for several chaotic systems. For certain systems this can be expressed in terms of the Selberg zeta function.

For a large class of ergodic systems the quantum ergodicity theorem holds, which (roughly speaking) states that almost all eigenfunctions become equidistributed in the semiclassical limit. Particular attention has been paid to the question of subsequences of exceptional, non-quantum ergodic eigenfunctions, and their counting function. Such eigenfunctions are for example bouncing-ball modes occurring in billiards with two parallel walls (like the stadium or the Sinai billiard). Also "scarred" eigenfunctions showing localization along unstable periodic orbits could give rise to a non-quantum ergodic subsequence of eigenfunctions. Furthermore, the rate by which the classical limit is approached has been studied.

We conclude by giving a short summary of the other topics studied by our group within the Schwerpunktprogramm.

1 Introduction

Today it is well–known that the generic systems in classical physics are not the standard "textbook systems", which are completely integrable, but the non–integrable ones which range from near-integrable to ergodic and even fully chaotic systems. The latter display a very strong dependence on the initial conditions, i.e., even extremely small changes in the initial conditions have exponentially growing effects on the time evolution of the system. The chaotic behaviour of such sytems arises from the non-linearity of the differential equations describing them, i.e., from the non–linearity of Hamilton's equations in the case of classical mechanics. In the following it is assumed that the classical system is described by a time-independent Hamiltonian $H(\mathbf{p}, \mathbf{q})$ which for systems with f degrees of freedom is defined on the phase space $(\mathbf{p}, \mathbf{q}) \in \mathbb{R}^f \times \mathbb{R}^f$. Here $\mathbf{q} \in \mathbb{R}^f$ denotes the coordinates and $\mathbf{p} \in \mathbb{R}^f$ the canonical momenta. The observables in classical mechanics are (smooth) functions $A(\mathbf{p},\mathbf{q})$ on phase space. In the following we shall assume that the Hamiltonian flow on the energy shell is (at least) ergodic; thus the energy $E = H(\mathbf{p},\mathbf{q})$ is the only constant of motion. Although such systems are fully deterministic, their time evolution may be practically unpredictable in the long–time limit, $t \to \infty$. Prototype examples of strongly chaotic systems are certain billiards, which are given by the free motion of a point particle with mass m inside a compact Euclidean domain Ω with elastic reflections at the boundary $\partial\Omega$, or by the geodesic motion on a compact Riemann surface with constant negative curvature, or by billiards on compact domains with constant negative curvature.

Modern physics is based on quantum mechanics which governs not only the world of atoms, molecules and elementary particles, but is also more fundamental than classical mechanics in that the latter can be obtained from it in the *semiclassical limit*, $\hbar \to 0$, where $\hbar$ denotes Planck's constant. The semiclassical limit is different from the classical limit, for which $\hbar$ is precisely equal to zero, because, in general, quantal functions are non–analytic in $\hbar$ as $\hbar \to 0$. The basic quantity in quantum mechanics is a certain complex function Ψ called probability amplitude or wave function associated with every quantum mechanical (pure) state. In the simplest case of a single particle the wave function $\Psi(\mathbf{q},t)$ gives the probability density $|\Psi(\mathbf{q},t)|^2$ of finding the particle at the point $\mathbf{q}$ and at time t, i.e., $\int_D |\Psi(\mathbf{q},t)|^2 \, \mathrm{d}^f q$ is the probability to find the particle at time t in a given domain $D \subset \Omega$. The state space of quantum mechanics is the Hilbert space $L^2(\Omega, \mathrm{d}^f q)$ where $\Omega \subset \mathbb{R}^f$ denotes the configuration space. The wave function Ψ is calculated from a differential equation, which for non–relativistic systems, i.e., for particles of low velocity, is the *Schrödinger equation*

$$\mathrm{i}\hbar \frac{\partial \Psi(\mathbf{q},t)}{\partial t} = \widehat{H} \Psi(\mathbf{q},t) \quad . \tag{1}$$

Here $\widehat{H}$ is a self-adjoint differential operator called the Hamiltonian or Schrödinger operator, which is obtained from the classical Hamiltonian $H(\mathbf{p},\mathbf{q})$ of the associated dynamical system. Obviously, the Schrödinger equation is a deterministic equation, since knowledge of Ψ at $t = t'$ implies its knowledge at all subsequent times $t'' > t'$. However, the interpretation of $|\Psi|^2$ as the probability density of an event is an indeterministic interpretation. It is a remarkable fact that the Schrödinger equation is a *linear* differential equation even for systems where the associated classical dynamics is non–linear. In the case of billiards on a compact domain Ω, the wave function $\Psi(\mathbf{q},t'')$ at time t'' evolving from the initial state at time t' with wave function $\Psi(\mathbf{q},t')$ is given by

$$\Psi(\mathbf{q},t'') = \sum_{n=1}^{\infty} c_n \psi_n(\mathbf{q}) \mathrm{e}^{-\frac{\mathrm{i}}{\hbar} E_n (t''-t')} \quad , \tag{2}$$

where $\psi_n(\mathbf{q})$ and E_n are the eigenfunctions and eigenvalues of the *stationary Schrödinger equation*

$$-\frac{\hbar^2}{2m}\Delta\psi_n(\mathbf{q}) = E_n\psi_n(\mathbf{q}) \quad , \qquad \mathbf{q} \in \Omega \quad , \tag{3}$$

$\psi_n \in L^2(\Omega, \mathrm{d}^f q)$, with the appropriate Dirichlet, Neumann or periodic boundary conditions on $\partial\Omega$. Here Δ denotes the Laplace-Beltrami operator, which on the Euclidean plane is the usual Laplacian. Due to the compactness of Ω, the quantal energy spectrum $\{E_n\}$ is purely discrete. The complex coefficients c_n in eq. (2) are given in terms of the initial wave function $\Psi(\mathbf{q}, t')$ at time t' by

$$c_n = \int\limits_{\Omega} \psi_n^*(\mathbf{q})\Psi(\mathbf{q}, t')\, \mathrm{d}^f q \tag{4}$$

and obey the normalization condition $\sum_{n=1}^{\infty} |c_n|^2 = 1$.

For Euclidean billiards the mathematical problem defined by eq. (3) is the well–known eigenvalue problem of the Helmholtz equation, which for example in two dimensions also describes the eigenfrequencies of a vibrating membrane or of flat microwave cavities.

Whereas in classically bounded conservative systems, which are chaotic, one of the most obvious properties of chaos manifests itself in the long-time behaviour, like the exponential decay of certain correlation functions for $t \to \infty$, their quantum mechanical counterparts do not display such a behaviour since the time-dependent wave function (2) is an almost periodic function for fixed $\mathbf{q}$. Thus with respect to the long-time behaviour it is commonly believed that there is no phenomenon in quantum mechanics, that could be called temporal quantum chaos, which can be considered as a direct manifestation of the chaotic classical motion in the corresponding quantum system. (See, however, the recent paper [1].) For this reason, most work in the field of *quantum chaos* [2] has not been devoted to the long-time asymptotics $t \to \infty$, but instead to the study of energy levels and eigenfunctions, in particular of their statistical properties. Thus one of the main research lines of quantum chaos is the search for fingerprints left on the quantum system, i.e., on $\{E_n\}$ and $\{\psi_n\}$, by its classical counterpart. Since such fingerprints are expected to be seen most clearly in the semiclassical limit, one is interested in the behaviour of the energy levels $\{E_n\}$ and wave functions $\{\psi_n\}$ in this limit, which for quantum billiards corresponds to the limit $E_n \to \infty$.

2 Spectral statistics and quantum chaos

One main point of our research programme was the search for universal statistical properties of energy spectra and eigenfunctions of quantum mechanical systems whose classical dynamics is chaotic. Let us start therefore by giving a short overview on the statistical behaviour of the spectrum of energy levels. Depending on the properties of the corresponding classical dynamical systems one expects a different behaviour of the spectral statistics: It has been conjectured that the energy level statistics of integrable systems can be described by a Poissonian random process [3]. In contrast, the statistics of classically strongly chaotic systems are conjectured to be given by the corresponding random matrix distributions [4], where the statistics of systems possessing only one anti-unitary symmetry (for example time-reversal invariance) should be described by the Gaussian orthogonal ensemble (GOE), and the statistics of systems without symmetry should be described by the Gaussian unitary ensemble (GUE). Random matrix theory (RMT) is by now a well established mathematical theory describing the properties of such ensembles of matrices [5]. However, although much effort has been spent on proving these conjectures, only in certain special cases rigorous results have been achieved. We will return to this point later.

Let us now define some statistical measures, which will be illustrated by numerical results for the integrable circle billiard and for the chaotic cardioid billiard (the domain Ω of these billiards is shown in figs. 12 and 13). In both cases the spectra of even symmetry of the desymmetrized systems have been used (for details see [6,7]).

The spectral staircase function $N(E)$ (mode number, integrated level density) is given by

$$N(E) := \#\{n \,|\, E_n \leq E\} \tag{5}$$

and counts the number of energy levels E_n below a given energy E. The function $N(E)$ can be separated into a mean smooth part $\overline{N}(E)$ and a fluctuating part, the *mode fluctuations* $N_{\text{fluc}}(E)$

$$N(E) = \overline{N}(E) + N_{\text{fluc}}(E) \quad . \tag{6}$$

For two-dimensional billiards with domain Ω, the mean behaviour $\overline{N}(E)$ is given by the generalized Weyl formula [8] ($\hbar = 2m = 1$, $E \to \infty$)

$$\overline{N}(E) = \frac{\mathcal{A}}{4\pi} E - \frac{\mathcal{L}}{4\pi}\sqrt{E} + \mathcal{C} \quad , \tag{7}$$

where $\mathcal{A}$ denotes the area of the billiard, and $\mathcal{L} := \mathcal{L}^- - \mathcal{L}^+$, where $\mathcal{L}^-$ and $\mathcal{L}^+$ are the lengths of the boundary $\partial\Omega$ with Dirichlet and Neumann boundary conditions, respectively. Fig. 1 shows $N(E)$ and $\overline{N}(E)$ for the first eigenvalues of the circle billiard and the cardioid billiard, respectively. One observes that (7) describes the mean behaviour of $N(E)$ very well even down to the ground state, despite of being an asymptotic result.

To compare the quantal spectra of different systems, one has to get rid of the system-dependent constants in $\overline{N}(E)$, which is achieved by *unfolding* the spectra by

$$x_n := \overline{N}(E_n) \quad , \qquad n = 1, 2, 3, \ldots \quad . \tag{8}$$

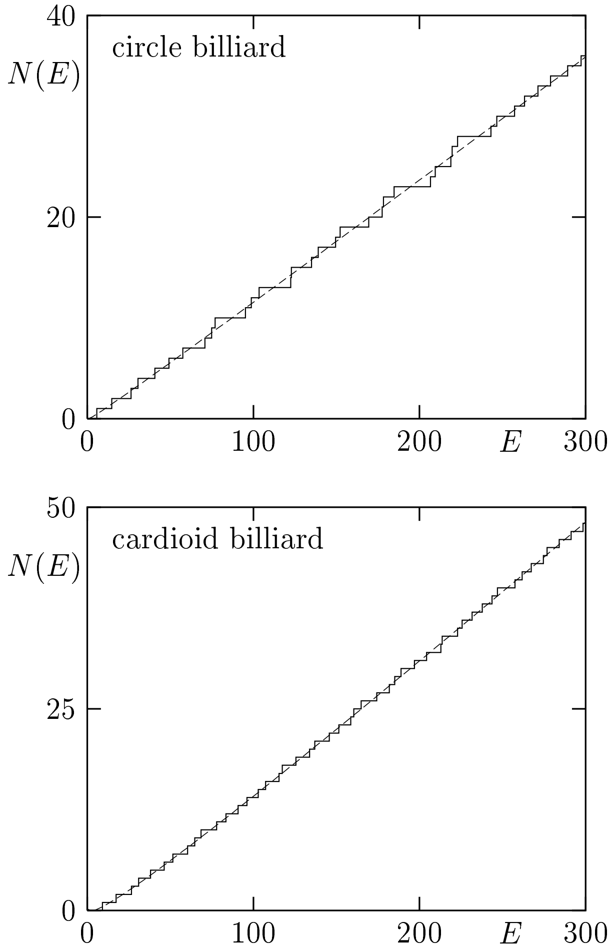

Fig. 1. Spectral staircase function $N(E)$ and its mean behaviour $\overline{N}(E)$, shown as dashed line, for the circle billiard and the cardioid billiard.

The unfolded spectrum $\{x_n\}$ has by construction a unit mean level spacing. In the sequel we will assume that the spectra are already unfolded, and in order to keep the notation simple, $N(x)$ will denote the spectral staircase of the unfolded energy spectrum, and $N_{\text{fluc}}(x)$ the corresponding fluctuating part. Thus $N(x) = x + N_{\text{fluc}}(x)$. Sometimes it is useful to include further long range oscillations in the unfolding procedure, see [7] for a detailed discussion.

To investigate the statistical distribution of quantum spectra, several statistical measures have been introduced. An important statistics is the nearest-neighbour level-spacing distribution $P(s)$ which is the probability density for the distribution of the distances $x_{n+1} - x_n$ between adjacent energy levels.

More precisely, the question is whether a limit distribution of $x_{n+1} - x_n$ exists in the following sense

$$\lim_{n\to\infty} \frac{\#\{i \le n \mid a \le x_{i+1} - x_i \le b\}}{n} = \int_a^b P(s)\,\mathrm{d}s \tag{9}$$

and of what shape $P(s)$ is.

According to the above–mentioned conjectures one expects for integrable systems

$$P_{\text{Poisson}}(s) = \mathrm{e}^{-s} \quad . \tag{10}$$

Since $P(s) \to 1$ for $s \to 0$ this behaviour is called *level attraction*.

The result of RMT for the level-spacing distribution is in the case of the GOE in very good approximation described by the Wigner distribution [5]

$$P_{\text{GOE}}(s) \approx P_{\text{Wigner}}(s) = \frac{\pi}{2} s \exp\left(-\frac{\pi}{4}s^2\right) \quad . \tag{11}$$

In the case of the GUE one has in very good approximation [5]

$$P_{\text{GUE}}(s) \approx \frac{32}{\pi^2} s^2 \exp\left(-\frac{4}{\pi}s^2\right) \quad . \tag{12}$$

In both cases we have $P(s) \to 0$ for $s \to 0$, which is called *level repulsion*.

To illustrate this behaviour, we show in fig. 2 the level-spacing distribution for the circle and for the cardioid billiard, respectively. The two distributions are in good agreement with the expected behaviour of a Poissonian random process and of the GOE, respectively, which was also observed for numerous other systems, see, e.g., [2] and references therein.

For long-range correlations the situation turns out to be more complicated. A convenient measure for medium- and long-range correlations is provided by the number variance $\Sigma^2(L, \hat{x})$, which is defined by

$$\Sigma^2(L, \hat{x}) := \left\langle [N(x+L) - N(x) - L]^2 \right\rangle_{\hat{x}} \quad , \quad L > 0 \quad , \tag{13}$$

which measures the variance of the number of eigenvalues in an energy interval of length L. Here the brackets denote an energy averaging for which there are a priori different possibilities. We choose the following rectangular averaging ($c > 1$)

$$\langle f(x) \rangle_{\hat{x}} := \frac{1}{(c-1)\hat{x}} \int_{\hat{x}}^{c\hat{x}} f(x)\,\mathrm{d}x \quad . \tag{14}$$

For a Poissonian random process one has

$$\Sigma^2_{\text{Poisson}}(L) = L \quad . \tag{15}$$

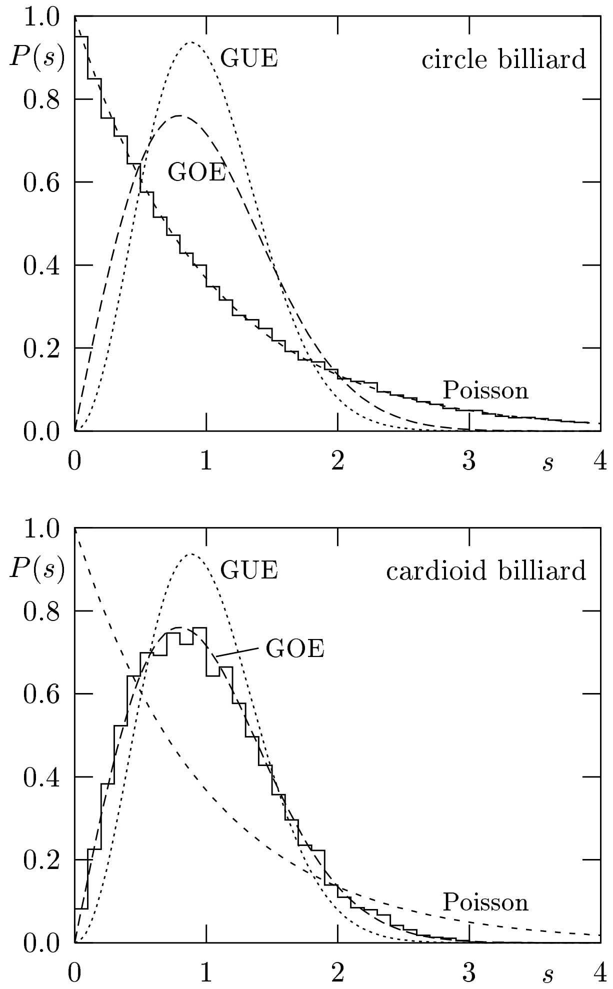

Fig. 2. Level–spacing distribution for the circle billiard (even symmetry, 100 000 eigenvalues) and the cardioid billiard (even symmetry, 11 000 eigenvalues).

In RMT one obtains in the case of the GOE [5]

$$\begin{aligned}\Sigma^2_{\mathrm{GOE}}(L) = \frac{2}{\pi^2}\Bigg\{&\ln(2\pi L) + \gamma + 1 + \frac{1}{2}\mathrm{Si}^2(\pi L) - \frac{\pi}{2}\mathrm{Si}(\pi L) \\ &- \cos(2\pi L) - \mathrm{Ci}(2\pi L) + \pi^2 L\left[1 - \frac{2}{\pi}\mathrm{Si}(2\pi L)\right]\Bigg\} \quad ,\end{aligned} \tag{16}$$

and for the GUE [5]

$$\Sigma^2_{\rm GUE}(L) = \frac{1}{\pi^2}\{\ln(2\pi L) + \gamma + 1 - \cos(2\pi L) - {\rm Ci}(2\pi L) + \pi^2 L\left[1 - \frac{2}{\pi}{\rm Si}(2\pi L)\right]\} \ , \tag{17}$$

where $\gamma = 0.5772\ldots$ is Euler's constant and ${\rm Si}(x)$ and ${\rm Ci}(x)$ are the sine and cosine integral, respectively. Notice that the results (15)–(17) are "stationary", i.e., they do not depend on the energy $\hat{x}$ around which the averaging is carried out according to (14).

Fig. 3 shows the number variance for the circle billiard and the cardioid billiard, respectively. For small values of L, i.e., for short–range correlations, one observes good agreement with the conjectured Poisson (15) and GOE (16) behaviour. However, for larger values of L one observes deviations of $\Sigma^2(L,\hat{x})$ from $\Sigma^2_{\rm Poisson}(L)$ and $\Sigma^2_{\rm GOE}(L)$, respectively, and the number variance fluctuates around a saturation plateau of height $\Sigma^2_\infty(\hat{x})$. Notice that the fluctuations are much larger for the integrable system, for which also the saturation plateau is higher than for the cardioid billiard.

The RMT results for large L are $\Sigma^2_{\rm GOE}(L) \sim \frac{2}{\pi^2}\ln(2\pi L)$ and $\Sigma^2_{\rm GUE}(L) \sim \frac{1}{\pi^2}\ln(2\pi L)$ which is in contrast to the observed saturation of the number variance, see, e.g., [9–14,6]. Berry has given a semiclassical argument for the saturation behaviour of the number variance [9] and of the spectral rigidity [15]. It turns out that with $L_{\max} := a\sqrt{\hat{x}}$, where $a > 0$ is a system-dependent constant, one has the universality regime for $L \ll L_{\max}$, in which the spectral statistics are expected to be described by random matrix theory. For $L \gg L_{\max}$, however, the number variance clearly deviates from the RMT result and rather oscillates around its saturation plateau $\Sigma^2_\infty(\hat{x})$. The saturation value $\Sigma^2_\infty(\hat{x})$ increases with increasing energy $\hat{x}$ in the limit of large $\hat{x}$.

However, the above presented picture does not always hold, as there are important exceptions to the generically expected behaviour. The general behaviour of chaotic systems is violated by systems possessing arithmetical chaos [13,16–22], where, e.g., the level-spacing distribution and the two-point statistics nearly behave as for classically integrable systems. Another example of a strongly chaotic system showing non–generic spectral statistics are quantized cat maps [23].

As an example for a class of integrable systems, the eigenvalue statistics for the geodesic flow on flat tori are studied in [24]. It is proven that the pair correlation function is Poissonian for a set of full Lebesgue measure in the parameter space of tori, whereas the consecutive level-spacing distribution does not exist for a set of second Baire category (a topologically large set). Explicit examples of tori with Poissonian pair correlation function are given in [25]. A further class of integrable systems showing exceptional behaviour are harmonic oscillators with irrational ratio of frequencies, for which the nearest–neighbour level–spacing distribution and other spectral statistics do not possess a limit distribution, see, e.g., [3,26–30] and references therein.

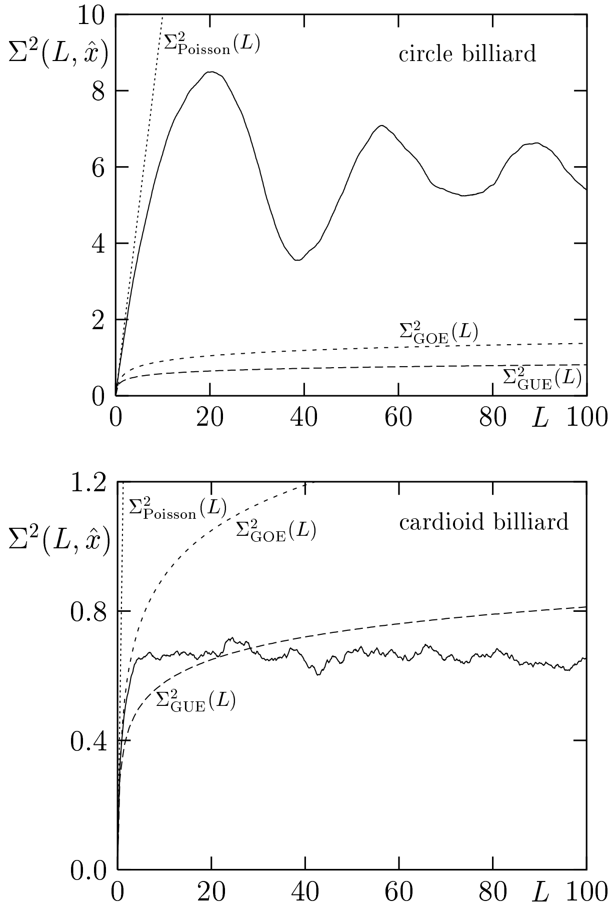

Fig. 3. Number variance for the circle and cardioid billiard for $\hat{x} = 1000$ and $c = 3$.

Recently it has been shown that for the class of quantized skew translations on the torus (also called parabolic maps) [31–33], which are ergodic but not mixing for irrational parameters, the spectral statistics do not possess a limit distribution [34].

As the standard spectral statistics do not always provide a measure to distinguish between integrable and chaotic systems, in particular even for systems as strongly chaotic as the geodesic motion on arithmetic surfaces of constant negative curvature, the distribution of the suitably normalized mode fluctuations have been proposed in [35,36] as an alternative statistical measure. Fig. 4 shows $N_{\text{fluc}}(x)$ for the first 3000 eigenvalues of the circle billiard and the cardioid billiard. Since $N_{\text{fluc}}(x)$ behaves very irregularly the idea is to consider $N_{\text{fluc}}(x)$ as a random function of x and to look for its statistical

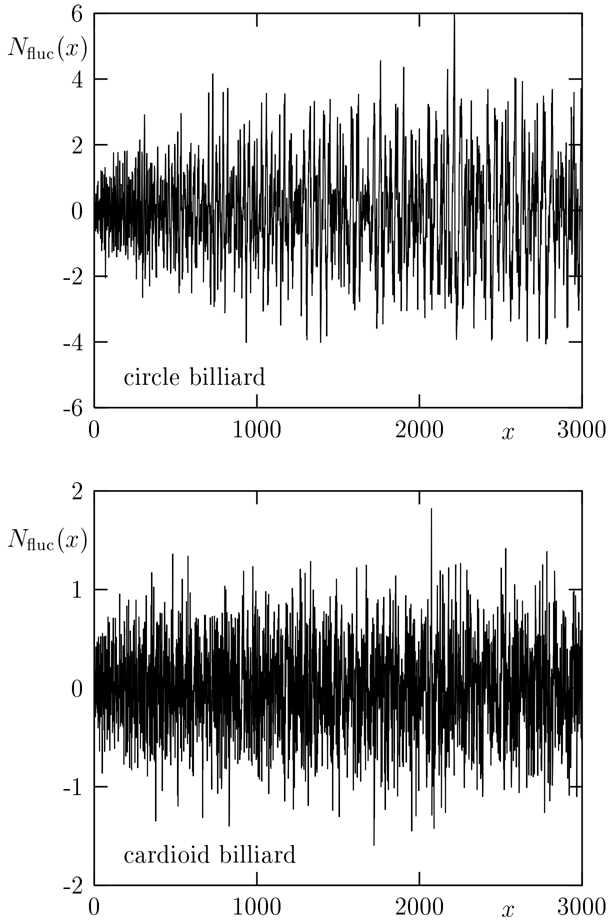

Fig. 4. Plot of $N_{\text{fluc}}(x)$ for the first 3000 eigenvalues of the circle billiard and the cardioid billiard. Notice that the fluctuations are much larger for the integrable system in comparison with the chaotic system.

properties. However, in fig. 4 one observes an increase in the amplitude of the fluctuations and thus $N_{\text{fluc}}(x)$ itself cannot possess a limit distribution. Therefore, one defines the variance

$$D(x) := \frac{\Xi(c)}{(c-1)\,x} \int\limits_x^{cx} [N_{\text{fluc}}(y)]^2 \, \mathrm{d}y \quad , \tag{18}$$

with $c > 1$, where $\Xi(c)$ is a constant ensuring normalization, see [7]. With this one can construct the following random variable

$$W(x) := \frac{N_{\text{fluc}}(x)}{\sqrt{D(x)}} \quad , \tag{19}$$

where x is randomly chosen from the interval $[T, cT]$. If a limit distribution of the random variable $W(x)$ exists for $T \to \infty$, it has by construction a second moment of one if the second moment exists. Furthermore, the first moment of this limit distribution is zero because $N_{\text{fluc}}(x)$ describes by definition the fluctuations of $N(x)$ around the mean behaviour $\overline{N}(x) = x$.

The conjecture proposed in [35,36] can now be formulated as follows:

Conjecture: *For bound conservative and scaling systems the quantity $W(x)$, eq. (19), $x \in [T, cT]$, possesses a limit distribution for $T \to \infty$. This distribution is absolutely continuous with respect to the Lebesgue measure on the real line, with a density $P(W)$*

$$\lim_{T\to\infty} \frac{1}{(c-1)\,T} \int\limits_T^{cT} g(W(x))\,\rho(x/T)\,\mathrm{d}x = \int\limits_{-\infty}^{\infty} g(W)\,P(W)\,\mathrm{d}W \quad , \tag{20}$$

where $g(x)$ is a bounded continuous function, and $\rho(t) \geq 0$ is a continuous density on $[1, c]$ with $\frac{1}{c-1}\int_1^c \rho(t)\,\mathrm{d}t = 1$.

Furthermore, the limit distribution has zero mean and unit variance,

$$\int\limits_{-\infty}^{\infty} W\,P(W)\,\mathrm{d}W = 0 \qquad , \qquad \int\limits_{-\infty}^{\infty} W^2\,P(W)\,\mathrm{d}W = 1 \quad . \tag{21}$$

If the corresponding classical system is strongly chaotic, having only isolated and unstable periodic orbits, then $P(W)$ is universally a Gaussian, $P(W) = \frac{1}{\sqrt{2\pi}}\exp(-\frac{1}{2}W^2)$. In contrast, a classically integrable system leads to a non-Gaussian density $P(W)$.

In the following we will consider two aspects only, for a detailed discussion see [36,7,37].

For classically chaotic systems a semiclassical approximation to $N_{\text{fluc}}(x)$ is given by means of Gutzwiller's periodic-orbit theory [2], see section 3. In this theory $N_{\text{fluc}}(x)$ can be expressed in terms of the *dynamical zeta function* $Z(s)$ which involves only properties of the periodic orbits like their lengths, stabilities and Maslov indices. The non-trivial zeros of the dynamical zeta function $Z(s)$ are directly connected with the quantal levels of the corresponding system. Using the argument principle, one obtains for two–dimensional billiards

$$\widetilde{N}_{\text{fluc}}(p) = \frac{1}{\pi}\arg Z(\mathrm{i}p) \quad . \tag{22}$$

(The tilde distinguishes $\widetilde{N}_{\text{fluc}}(p)$, which is a function of the momentum $p = \sqrt{E}$, from $N_{\text{fluc}}(x)$ which is a function of the unfolded energy x.)

An interesting number theoretical example is provided by the non-trivial zeros of the Riemann zeta function $\zeta(s)$. Their statistics behave in many respects like the eigenvalues of some hypothetical classically chaotic system without anti-unitary symmetry. Here one has

$$\widetilde{N}_{\text{fluc}}(p) = \frac{1}{\pi} \arg \zeta \left(\frac{1}{2} + \mathrm{i}p \right) \quad , \tag{23}$$

where $\widetilde{N}_{\text{fluc}}(p)$ is the fluctuating term of the counting function $N(p)$, which counts the non–trivial Riemann zeros ρ_n, $\zeta(\rho_n) = 0$ with $0 < \operatorname{Re} \rho_n < 1$ and $0 < \operatorname{Im} \rho_n \leq p$. It can be shown that for a certain class of zeta functions, which includes the Riemann zeta function, the corresponding normalized fluctuations (given here for the Riemann zeta function)

$$\widetilde{W}(p) = \frac{\widetilde{N}_{\text{fluc}}(p)}{\sqrt{\frac{1}{2\pi^2} \ln \ln p}} \tag{24}$$

have indeed a Gaussian limit distribution [38–40].

For integrable systems a lot of results concerning the limit distribution $P(W)$ of $W(x)$ have been obtained, see [7,37,41,42] for summaries. For several completely integrable two–dimensional geodesic flows it is possible to show

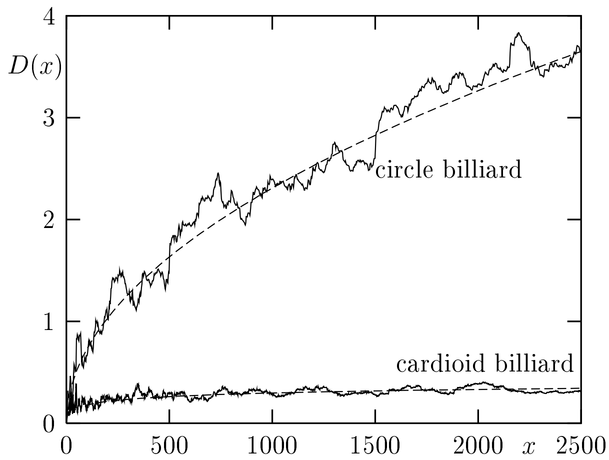

Fig. 5. Plot of the variance $D(x)$ for the circle billiard and the cardioid billiard using $c = 1.1$. Also shown (dashed curves) are the expectations based on semiclassical arguments [15], which lead [20,36] to $D(x) \sim C\sqrt{x}$ for the integrable case and $D(x) \sim \frac{1}{2\pi^2} \ln x + C'$ for the chaotic (GOE) case.

that $N(E)$ can be decomposed as follows (see eqs. (5) and (7))

$$N(E) = \frac{\mathcal{A}}{4\pi}\, E + E^{1/4}\ \Theta(\sqrt{E}) \ \ , \tag{25}$$

where the remainder term $E^{1/4}\ \Theta(\sqrt{E})$ fluctuates around zero with an amplitude increasing as $E^{1/4}$ and is identified with $N_{\rm fluc}(E)$. The first term is the Weyl term. Since the considered systems have no boundary, there is no additional term involving $\mathcal{L}$, and also the constant $\mathcal{C}$ in (7) is zero. It could be shown that eq. (20) holds and, furthermore, that the corresponding limit distribution decays faster than a Gaussian. The basic idea for proving the existence of a limit distribution of $\Theta(\sqrt{E})$ is to express $N(E)$ in terms of a sum over periodic orbits, or (equivalently) to reduce $N(E)$ to a lattice-point problem and then to exploit the Poisson summation formula to obtain an expression of the remainder term as a trigonometric series. If the remainder term is an *almost periodic function* [43] then it has a limit distribution [44]. A simple example is given by the eigenvalues of the Laplacian on a two-dimensional torus. The eigenvalues read (in suitable units) $E_{n,m} = n^2 + m^2$ with $n, m \in \mathbb{Z}$. Thus to determine $N_{\rm fluc}(E)$ one is led to the *classical circle problem*, due to Gauß, where one considers the difference between the number of lattice points inside a circle of radius $R = \sqrt{E}$ and the corresponding area πR^2. For a long time one was concerned with finding optimal estimates of the form $O(E^\alpha)$ for the error term $N(E) - \pi\, E$. Gauß proved $\alpha = \frac{1}{2}$ which follows from the fact that the remainder term cannot grow faster than the length of the boundary. Hardy's conjecture [45] that $\alpha = \frac{1}{4} + \varepsilon$ for all positive ε is still unproven. Probably the best estimate at the present time is $|N(E) - \pi\, E| \leq C_\varepsilon E^{23/73} (\log E)^{315/146}$ [46]. It was Heath-Brown [47] who had the idea to study the probabilistic properties of $\Theta(\sqrt{E})$, see eq. (25), instead of obtaining an optimal value for α. In the case of the circle problem he was then able to prove that $\Theta(R)$ possesses a limit distribution.

Before we turn to the $P(W)$ distribution, we present in figure 5 the variance $D(x)$ for the circle and cardioid billiard using the first 11 000 levels and $c = 1.1$, see eq. (18). For the integrable system one observes that the variance of $N_{\rm fluc}(x)$ is much larger than for the chaotic system, for which $D(x)$ increases only logarithmically. Fig. 6 shows the mode–fluctuation distribution $P(W)$ for the cardioid billiard and the stadium billiard (for which also the contribution of the bouncing ball orbits has been included in the unfolding procedure, see [7] for details). In both cases very good agreement with the Gaussian normal distribution (shown as dashed line) is observed. It should be emphasized that this is even true for the arithmetic systems [36,13,7], for which the usual spectral statistics, like the level-spacing distribution, show strong deviations from the expected GOE behaviour.

For comparison, fig. 7 shows the mode–fluctuation distribution $P(W)$ for a) a triangular billiard, b) the circle billiard, c) the torus and d) a rectangular billiard [7]. In accordance with the conjecture and the analytical results, for

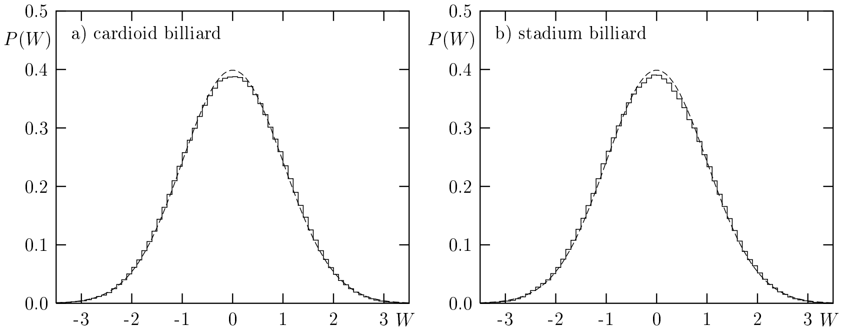

Fig. 6. Mode–fluctuation distribution $P(W)$ for the cardioid billiard and the stadium billiard in comparison with the Gaussian normal distribution (dashed curve).

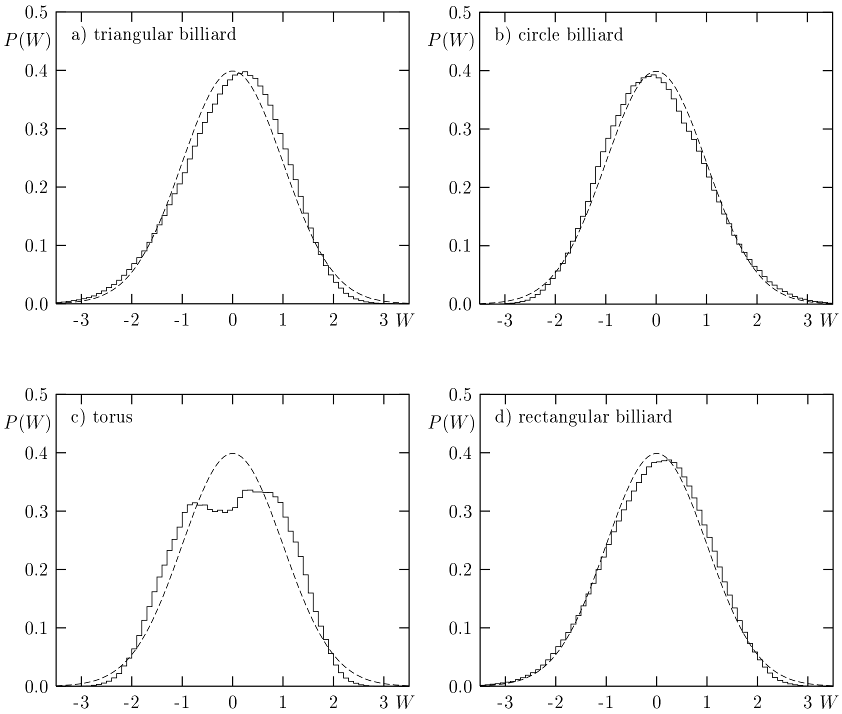

Fig. 7. Mode–fluctuation distribution $P(W)$ for four integrable billiards in comparison with the Gaussian normal distribution (dashed curve).

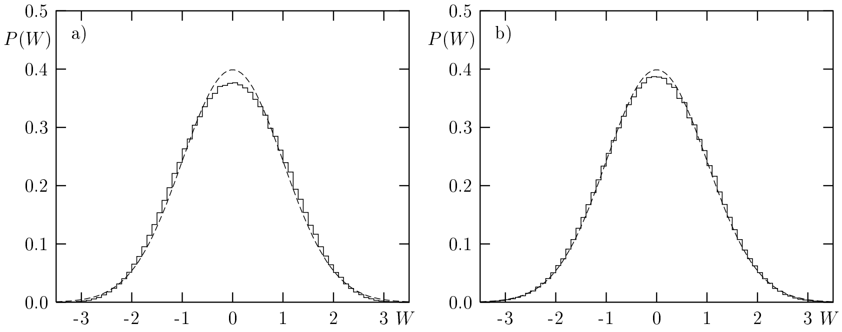

Fig. 8. Mode–fluctuation distribution for the Riemann zeta function, computed according to (24) a) for the first 50 000 zeros and b) for 50 000 zeros starting from the $10^{20} + 143\,780\,420$th zero.

these integrable systems clear deviations from the Gaussian behaviour are observed.

Finally we show in fig. 8 the mode–fluctuation distribution for the Riemann zeta function which has been computed [48] according to (24) from the non-trivial zeros [49]. Notice that the convergence to the (proven) Gaussian limit distribution is very slow.

In [50] the mode–fluctuation distribution $P(W)$ has been analyzed for experimentally measured spectra of several two– and three–dimensional superconducting microwave cavaties in the frequency range below 20 GHz. For the stadium billiard and the 3D–Sinai billiard it is found that $P(W)$ is in good agreement with our conjecture.

For the integrable geodesic flow on Riemannian manifolds all of whose geodesics are closed a trace formula has been derived in [51] and it has been shown that $P(W)$ is a box-shaped function and thus different from a Gaussian which is again in accordance with our conjecture.

3 Trace formulae and symbolic dynamics

A fundamental formula which relates the energy levels of a given quantum system to properties of the corresponding classical dynamical system is provided by the Gutzwiller trace formula [52,2]. This formula gives a formal semiclassical expression for the quantum mechanical density of states as a sum over periodic orbits. With $\hbar = 2m = 1$, $d(p) := \frac{\mathrm{d}N(E=p^2)}{\mathrm{d}p} = 2pd(E=p^2) = \sum_n \delta(p - p_n)$, $p > 0$, $p_n = \sqrt{E_n}$, and the mean behaviour $\bar{d}(p) := \frac{\mathrm{d}\bar{N}(E=p^2)}{\mathrm{d}p}$, the *Gutzwiller trace formula* reads for two–dimensional, strongly chaotic billiards (i.e., all orbits are isolated and unstable)

$$d(p) \sim \bar{d}(p) + d_{\text{fluc}}(p) = \bar{d}(p) + \frac{1}{\pi} \sum_{\gamma} \sum_{k=1}^{\infty} \frac{l_\gamma \cos\left(k l_\gamma p - \frac{\pi}{2} k \nu_\gamma\right)}{\sqrt{|2 - \operatorname{Tr} M_\gamma^k|}} \tag{26}$$

for $p \to \infty$. Here γ denotes the primitive periodic orbits, and the k-summation accounts for their multiple traversals. l_γ is the geometric length of the primitive periodic orbit γ and ν_γ denotes the Maslov index, see below. $\operatorname{Tr} M_\gamma$ is the trace of the monodromy matrix M_γ of the primitive periodic orbit γ where M_γ is obtained from the linearization of the flow around the orbit.

As for chaotic systems the number of periodic orbits up to a given length is expected (and for several systems known) to grow exponentially, the sum on the right hand side in eq. (26) is not absolutely convergent, see [53,54]. For systems with only even Maslov indices ν_γ, generalized periodic orbit sum rules have been derived, which involve absolutely convergent sums and integrals only [54]. In [54] the test function $h(p)$ is assumed to fulfil the following three conditions:

a) $h(p)$ is even in p

b) $h(p)$ is analytic in the strip $|\operatorname{Im} p| \leq \sigma + \epsilon$, $\epsilon > 0$

c) $|h(p)| \leq a|p|^{-2-\delta}$ with $\delta > 0$, $a > 0$ for $|p| \to \infty$,

with $\sigma = h_{\text{top}}^{\text{flow}} - \overline{\lambda}/2$, where $h_{\text{top}}^{\text{flow}}$ is the topological entropy of the Hamiltonian flow and $\overline{\lambda}$ is a "mean Lyapunov exponent" [54]. In general one has $\sigma = P(\frac{1}{2}) > 0$, where $P(\beta)$ is the topological pressure, see [37] for details.

Including also the case of odd Maslov indices ν_γ, the generalized periodic orbit sum rules read [54,6]

$$\sum_n h(p_n) \sim \int_0^\infty h(p')\bar{d}(p') \, \mathrm{d}p' + \mathcal{C}h(0) + \sum_\gamma \sum_{k=1}^\infty \frac{l_\gamma}{\sqrt{|2 - \operatorname{Tr} M_\gamma^k|}} \mathcal{F}_\gamma\{h(kl_\gamma)\} \ , \tag{27}$$

where

$$\mathcal{F}_\gamma\{h(x)\} := \frac{1}{\pi} \int_0^\infty h(p') \cos\left(xp' - \frac{\pi}{2} k\nu_\gamma\right) \, \mathrm{d}p' \ , \tag{28}$$

and $\mathcal{C}$ is the constant in the generalized Weyl formula, eq. (7). Formally one can obtain this result by multiplying both sides of eq. (26) by a test function $h(p)$ and integrating over p from 0 to ∞.

In the mathematical literature similar trace formulae have been derived by Colin de Verdière [55,56], Chazarain [57] and Duistermaat and Guillemin [58] in the context of pseudodifferential and Fourier integral operators. For the connection to Schrödinger operators see [59–62].

The first example of a trace formula which is even exact and not just a semiclassical approximation is the Selberg trace formula which applies to certain manifolds with constant negative curvature. The associated dynamical systems play an important role in ergodic theory and in the study of quantum chaos. Our group has extensively studied these systems and the Selberg trace formula in a series of papers, see, e.g., [10,12,13,16,17,19,20,22,63–71].

Trace formulae play an important role in the attempts to understand the statistical properties of energy levels. Using trace formulae the spectral fluctuations can be expressed in terms of periodic orbit sums and are thus strongly linked to the correlations in the length spectra of periodic orbits.

Using appropriate test functions $h(p)$ one can get information on the classical length spectrum using the quantum mechanical energy levels. Conversely, one may use the periodic orbits to compute energy levels which thus provides a substitute for the WKB– and EBK–formulae, which can be applied to integrable systems only.

In fig. 9 we illustrate how the lengths l_γ of the shortest periodic orbits can be obtained from the quantal energy levels. This is done by a Fourier analysis of the quantum mechanical density of states. For the choice [63,64,72]

$$h(p) = \cos(pL)\,\mathrm{e}^{-p^2 t}\,; \qquad p = \sqrt{E}\ , \quad t > 0\ , \qquad L \in \mathbb{R}\ , \qquad (29)$$

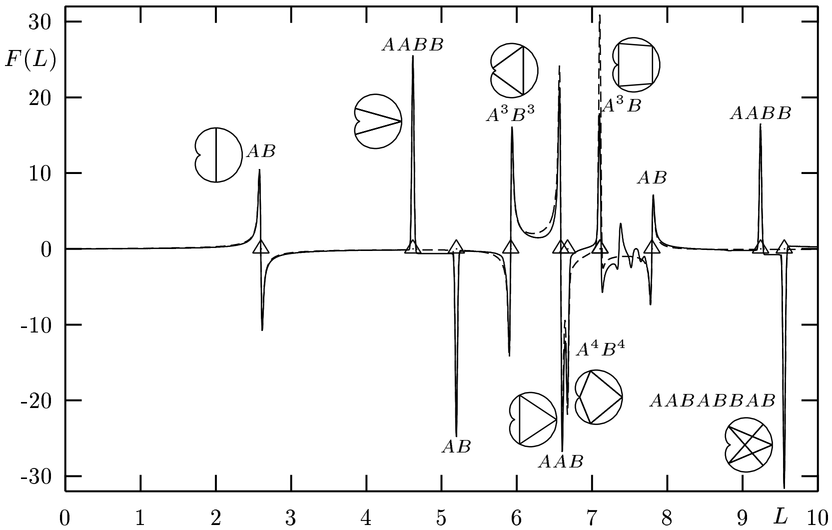

Fig. 9. The trace of the cosine–modulated heat kernel for the cardioid billiard is shown (eigenvalues of odd symmetry). The full line is $F(L)$, eq. (32), with $n_{\max} = 11000$, $t = 0.0001$, and the dashed line shows the semiclassical result $F_{\rm sc}(L)$, eq. (33), using the periodic orbits up to geometric length 10. The triangles mark the lengths l_γ of the shortest periodic orbits in the desymmetrized system. Also shown are the corresponding orbits in the full cardioid billiard together with their symbolic code.

as test function in eq. (27) one obtains the so-called *trace of the cosine-modulated heat kernel*, $\mathrm{Tr}\{\cos\left((-\Delta)^{1/2}L\right) e^{t\Delta}\}$. The parameter t determines a smooth cut–off allowing for a suppression of the oscillations occurring for a sharp cut–off. The test function (29) yields for the right–hand side of (27) for even $k\nu_\gamma = 2m$ [63]

$$\mathcal{F}_\gamma\{h(x)\} = \frac{(-1)^m}{4}\frac{1}{\sqrt{\pi t}}\left[\exp\left(-\frac{(x-L)^2}{4t}\right) + \exp\left(-\frac{(x+L)^2}{4t}\right)\right] \quad , \tag{30}$$

whereas for odd $k\nu_\gamma = 2m+1$ one obtains [6]

$$\begin{aligned}\mathcal{F}_\gamma\{h(x)\} = \frac{(-1)^m}{4}\frac{1}{\pi t}\Bigg[&(x-L)\,{}_1F_1\left(1,\frac{3}{2},-\frac{(x-L)^2}{4t}\right)\\ &+(x+L)\,{}_1F_1\left(1,\frac{3}{2},-\frac{(x+L)^2}{4t}\right)\Bigg] \quad ,\end{aligned} \tag{31}$$

where ${}_1F_1(a,b,z)$ is Kummer's function [73].

In fig. 9 we show a plot of the trace of the cosine–modulated heat kernel where we have subtracted the mean behaviour from the left–hand side of (27). This gives [6,13]

$$F(L) := \sum_{n=1}^{n_{\max}} \cos(p_n L)\,\mathrm{e}^{-p_n^2 t} - \int\limits_0^{p_{\max}} \cos(pL)\,\mathrm{e}^{-p^2 t}\bar{d}(p)\,\mathrm{d}p - \mathcal{C} \quad , \tag{32}$$

where $n_{\max}$ is the index of the largest available eigenvalue and $p_{\max} = \sqrt{E_{n_{\max}}}$. The function $F(L)$ has to be compared with the semiclassical expression according to the trace formula (27)

$$F_{\mathrm{sc}}(L) := \sum_\gamma \sum_{k=1}^{\infty} \frac{l_\gamma}{\sqrt{|2-\mathrm{Tr}M_\gamma^k|}}\,\mathcal{F}_\gamma\{h(kl_\gamma)\} \quad . \tag{33}$$

One observes a very good agreement between both sides of the trace formula. The periodic orbits corresponding to the peaks are also shown, together with their symbolic code (see below).

As a second example for the application of trace formulae we consider the *cosine quantization rule*[66,74]. Using a semiclassical expression $N_{\mathrm{sc}}(E)$ for the staircase function $N(E)$ according to the semiclassical trace formula (26), an efficient quantization rule for the determination of semiclassical approximations to the eigenvalues is given by the zeros of the function $f(E)$,

$$f(E) := \cos\left(\pi N_{\mathrm{sc}}(E)\right) = 0 \quad . \tag{34}$$

Fig. 10 shows $f(E)$ for the cardioid billiard (odd symmetry), where all periodic orbits up to code length 20 have been included in the sum over periodic orbits. The triangles correspond to the exact eigenvalues, and one observes very good overall agreement between the zeros of $f(E)$ and the eigenvalues; for the first 31 eigenvalues the average error in units of the mean level spacing is 5.7%, see [75] for a detailed analysis.

From the above examples it is clear that for a thorough understanding of the properties of a given quantum system a detailed knowledge of the periodic orbits of the corresponding classical system is necessary. One of the best approaches to determine the periodic orbits is to find a symbolic dynamics for the system. Roughly speaking, a symbolic dynamics gives a labelling of trajectories of a given system by means of bi-infinite symbol sequences. Periodic orbits correspond to periodic symbol sequences and can thus be searched for in a systematic way. In particular for billiards a lot of results in this direction have been obtained leading to so-called Markov partitions. For non-uniformly hyperbolic billiard systems with singularities, Markov partitions are usually countably infinite, see, e.g., [76–79]. However, if one is interested in a symbolic description of trajectories, it is already sufficient and even more appropriate to find a finite generating partition (see, e.g., [80]), without the need for the Markov property.

In [81] the existence of finite generating partitions for a large class of two–dimensional hyperbolic maps with singularities is proven. The (explicit) construction is based on a partition determined by the singularity lines of the map, which is shown to be generating. This result applies for example to the cardioid billiard, to dispersing and semidispersing billiards and to

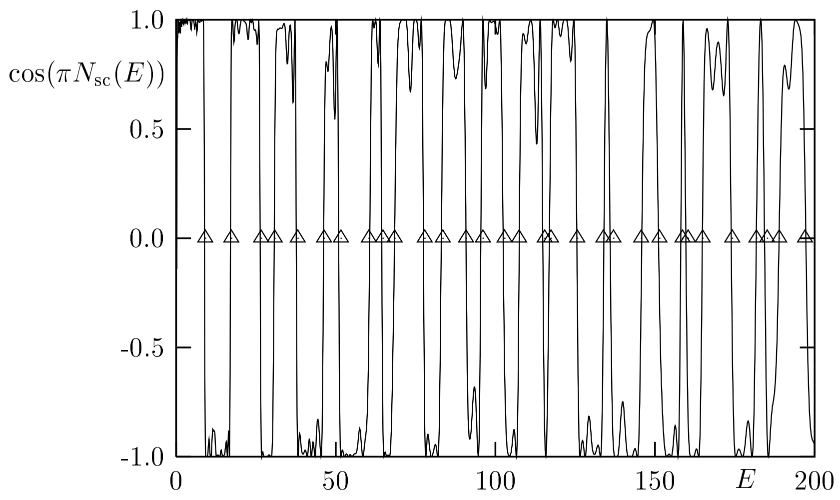

Fig. 10. Cosine quantization rule using the unsmoothed semiclassical spectral staircase function for the cardioid billiard (odd symmetry). All orbits up to code length 20 have been taken into account. The triangles mark the exact eigenvalues E_n.

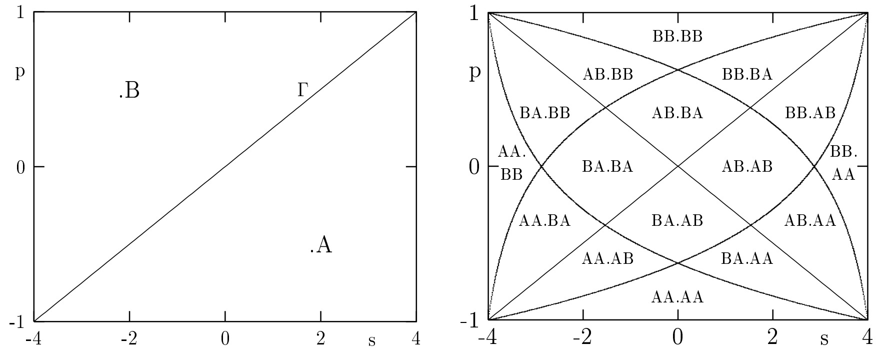

Fig. 11. Initial partition of the Poincaré section $\mathcal{P}$ for the cardioid billiard which is given by the two symbols A and B separated by the singularity line Γ. The figure to the right shows a refined partition where four symbols are fixed.

Bunimovich billiards. In particular for the stadium billiard this gives a proof of a previously conjectured symbolic dynamics [82].

Instead of giving the general statement, we would like to illustrate the result for the cardioid billiard, where the symbolic dynamics is given in terms of two symbols [83,84]. The boundary of the cardioid billiard is given in polar coordinates by $\rho(\varphi) = 1 + \cos\varphi$ with $\varphi \in [-\pi, \pi]$. The usual Poincaré section is given by $\mathcal{P} = \{(s,p) \mid s \in [-4,4],\ p \in [-1,1]\}$, where $s = 4\sin(\varphi/2)$ is the arclength coordinate along the boundary and p is the projection of the unit velocity vector (after the reflection at the boundary) on the tangent in the point of the billiard boundary corresponding to s. The normalized invariant measure of the billiard map $P : \mathcal{P} \to \mathcal{P}$ is given by $\mathrm{d}\mu = \frac{1}{16}\mathrm{d}s\,\mathrm{d}p$. In these coordinates the singularity line of P, i.e., the set of points which will hit the cusp of the cardioid in the next iteration, is simply given by $\Gamma = \{(s,p) \mid p = s/4,\ s \in [-4,4]\}$. This leads to a partition of $\mathcal{P}$ into two regions A and B as shown in fig. 11 [84]. Also shown is an example of a refined partition, where four symbols are fixed, giving altogether 16 cells. However, when fixing $2n$ symbols with $n \geq 5$ it turns out that not all symbol sequences are realized by the dynamical system, i.e., the number of cells of the refined partition is smaller than 2^{2n}. This has been called "pruning" of symbol sequences from the binary tree of possible combinations of letters A and B. A description of the set of forbidden symbol sequences has been proposed in terms of the so–called pruning front in the symbol plane [85]. This conjecture has been tested successfully for the cardioid billiard [84,75]. For certain model systems some progress in proving the pruning front conjecture has been made recently [86,87]. However, for the cardioid and other billiard systems this problem is still open.

4 Eigenfunctions and quantum ergodicity

The behaviour of the underlying classical system has also important consequences on the structure of the quantum eigenfunctions. A commonly used description of a quantum mechanical state is the Wigner function [88],

$$\mathrm{W}(\mathbf{p},\mathbf{q}) = \int\limits_{\mathbb{R}^2} \mathrm{e}^{\mathrm{i}\mathbf{q}'\mathbf{p}}\ \psi^\star\left(\mathbf{q}-\frac{\mathbf{q}'}{2}\right)\psi\left(\mathbf{q}+\frac{\mathbf{q}'}{2}\right)\,\mathrm{d}^2q' \ . \tag{35}$$

The Wigner function can be seen as a phase space representation of the wave function. It is not a probability density, as it may also take negative values. According to the "semiclassical eigenfunction hypothesis" the Wigner function semiclassically concentrates on those regions in phase space, which a generic orbit explores in the long–time limit $t \to \infty$ [89–91]. Therefore, in integrable systems the Wigner function $W(\mathbf{p},\mathbf{q})$ is expected to localize on the invariant tori. In fact, WKB constructions give so–called "quasimodes" [92–95], which localize in the semiclassical limit on the invariant tori. However, it is not guaranteed that a quasimode approximates an eigenfunction of the system, as is nicely seen in the well-known example of the double well potential, see, e.g., [95, §33, pp. 236].

For ergodic systems the semiclassical eigenfunction hypothesis implies that the Wigner function should semiclassically condense on the energy surface, i.e., $W(\mathbf{p},\mathbf{q}) \sim \frac{1}{\mathrm{vol}(\Sigma_E)}\,\delta(H(\mathbf{p},\mathbf{q})-E)$, where $H(\mathbf{p},\mathbf{q})$ is the Hamilton function and $\mathrm{vol}(\Sigma_E)$ is the volume of the energy shell defined by $H(\mathbf{p},\mathbf{q}) = E$. In fact this is the correct picture for "almost all" eigenfunctions. This follows from the quantum ergodicity theorem [96–102] (see also [21,103] for general introductions), which roughly speaking states that for almost all eigenfunctions the expectation values of quantum observables tend to the mean value of the corresponding classical observable in the semiclassical limit. "Almost all" means that this holds for a subsequence $\{\psi_{n_j}\} \subset \{\psi_n\}$ of density one, i.e.,

$$\lim_{E\to\infty} \frac{\#\{n_j \mid E_{n_j} \le E\}}{\#\{n \mid E_n \le E\}} = 1 \ . \tag{36}$$

As shown in [104], the quantum ergodicity theorem is equivalent to the validity of the semiclassical eigenfunction hypothesis for a subsequence of eigenfunctions of density one if the classical system is ergodic.

As an example consider as an observable the characteristic function χ_D of a domain $D \subset \Omega$. The quantum ergodicity theorem implies that in case the classical flow is ergodic, there exists a subsequence $\{\psi_{n_j}\} \subset \{\psi_n\}$ of density one, such that

$$\lim_{j\to\infty} \int\limits_D |\psi_{n_j}(\mathbf{q})|^2\ \mathrm{d}^2q = \frac{\mathrm{vol}(D)}{\mathrm{vol}(\Omega)} \tag{37}$$

for every measurable subset $D \subset \Omega$. So for almost all eigenfunctions the probability of finding a particle in a certain region D of the position space Ω becomes proportional to the volume D if the energy E becomes large.

More precisely the quantum ergodicity theorem can be formulated in terms of pseudo–differential operators (see, e.g., [105–108]) as follows:

Quantum ergodicity theorem [102]:

Let $\Omega \subset \mathbb{R}^2$ be a compact two-dimensional domain with piecewise smooth boundary, and let $\{\psi_n\}$ be an orthonormal set of eigenfunctions of the Dirichlet Laplacian $-\Delta$ on Ω. If the classical billiard flow on the energy shell $\Sigma_1 = S^1 \times \Omega$ is ergodic, then there is a subsequence $\{n_j\} \subset \mathbb{N}$ of density one such that

$$\lim_{j\to\infty} \langle \psi_{n_j}, A\psi_{n_j} \rangle = \int\limits_{\Sigma_1} \sigma(A)\, \mathrm{d}\mu \quad , \tag{38}$$

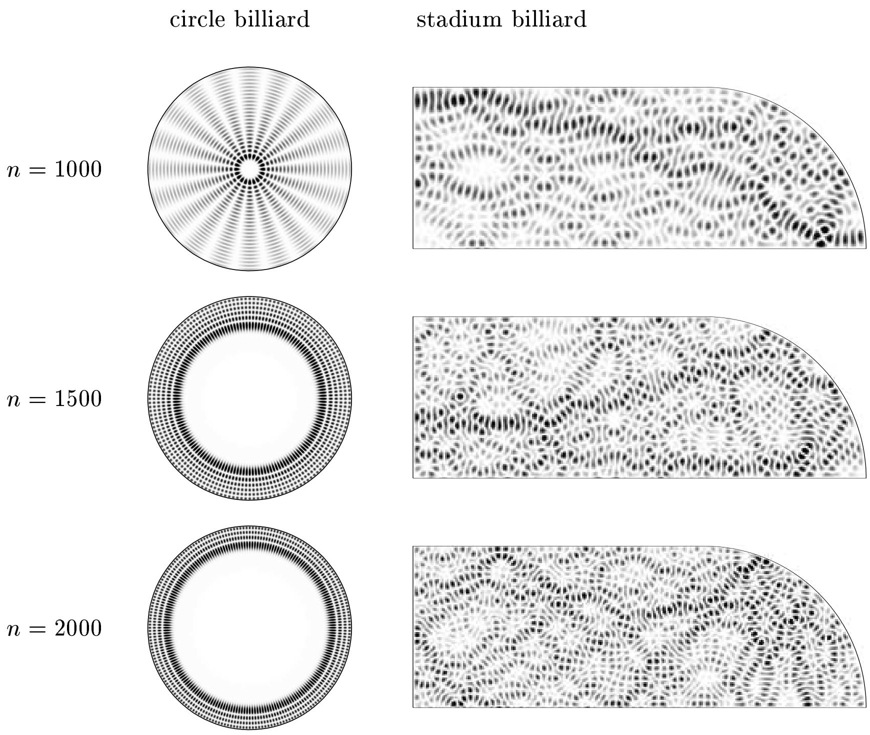

Fig. 12. Density plots of $|\psi_n(\mathbf{q})|^2$ for some eigenfunctions of the integrable circle billiard and the chaotic stadium billiard. Large values are encoded in black, and small values correspond to white.

for every classical pseudodifferential operator A of order zero, whose Schwartz kernel $K_A(\mathbf{q},\mathbf{q}') = \langle \mathbf{q}|A|\mathbf{q}'\rangle$ has support in the interior of $\Omega \times \Omega$. Here $\sigma(A)$ is the principal symbol of A and the average of $\sigma(A)$ is taken over the energy shell Σ_1 with respect to the Liouville measure μ.

The quantum ergodicity theorem does not just hold for two–dimensional Euclidean domains, but holds also for compact Riemannian manifolds without boundary [96,99,98,97], and a similar statement is true for systems where the Hamilton operator and the observables depend explicitly on $\hbar$ [100]. Also for certain quantized ergodic area–preserving maps on the torus the equipartition of eigenfunctions is proven [109,31,110].

The sequence of expectation values $\langle \psi_{n_j}, A\psi_{n_j}\rangle$ defines (roughly speaking) a sequence of measures on the energy shell, see, e.g., [104] for details. The limit points of this sequence of measures are called *quantum limits.* The special situation that there is only one quantum limit, i.e., the Liouville measure, is called *unique quantum ergodicity.* This behaviour is conjectured to be true for the eigenfunctions of the Laplacian on a compact manifold of negative curvature [112]. This conjecture is supported by a number of previous numerical studies, see, e.g., [67,113,71,114]. Recently it has been shown that quantized skew translations, which are uniquely ergodic, but not mixing for irrational parameters, are also quantum unique ergodic [33].

Fig. 12 illustrates the situation in position space for eigenfunctions of the integrable circle billiard and of the chaotic stadium billiard, respectively. The eigenfunctions of the circle billiard resemble the caustics obtained from the projection of the tori in phase space on position space, whereas the eigenfunctions of the stadium billiard look irregular for sufficiently large n.

However, one also observes so–called scarred eigenfunctions in the stadium and the cardioid billiard, which show localization along unstable periodic orbits [115–117,111], see fig. 13 for an example. This localization is not in contradiction to the quantum ergodicity theorem, as it only makes a statement about almost all eigenfunctions and therefore does not exclude the existence of eigenfunctions behaving differently. The degree of localization of an eigenfunction is also reflected in its maximum norm $||\psi||_\infty$. This has been studied in detail in [117], where numerical results for the maximum norms for several chaotic systems were found to agree with the expectation obtained from a random wave model for the eigenfunctions. This suggests that localization phenomena in exceptional sequences of eigenfunctions are weak.

Another candidate for a non–quantum ergodic subsequence of eigenfunctions are the so-called bouncing ball (bb) modes which occur in billiards with two parallel walls (like the stadium billiard or the Sinai billiard). These eigenfunctions are localized on the rectangular part of the billiard, see fig. 14 for some examples in the stadium billiard. The quantum ergodicity theorem gives

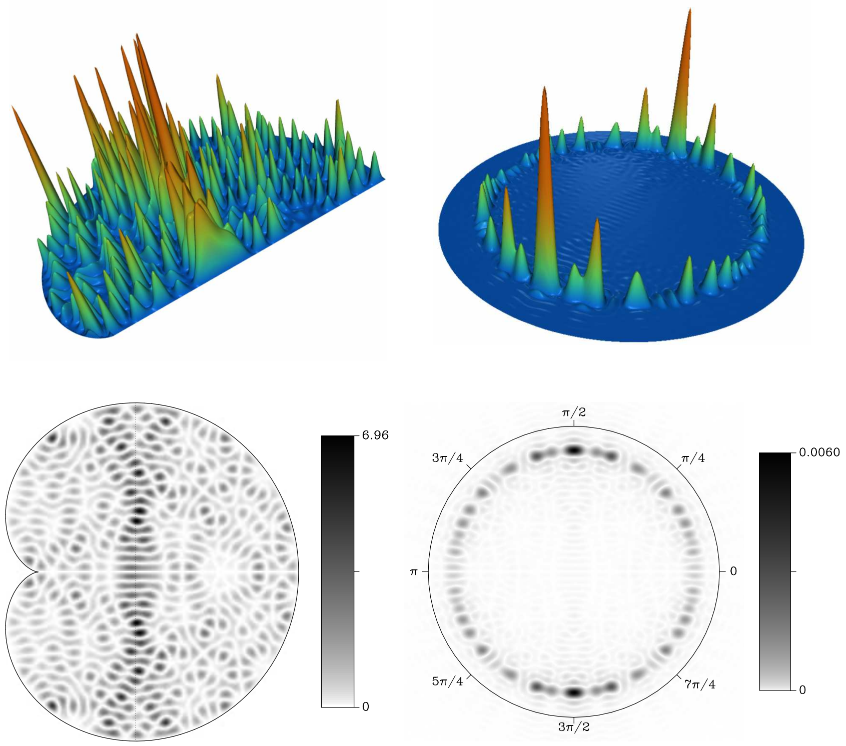

Fig. 13. Example of an eigenfunction showing localization along the shortest unstable periodic orbit AB. The left column shows a three-dimensional plot of $|\psi_{344}(\mathbf{q})|^2$ for the desymmetrized cardioid billiard (odd symmetry) and the corresponding density plot. In the right column a three dimensional plot of the momentum distribution $|\widehat{\psi}_{344}(\mathbf{p})|^2$ and the corresponding density plot is shown, see [111] for details. Here large values of $|\widehat{\psi}_{344}(\mathbf{p})|^2$ in some radial direction correspond to eigenstates with strong localization in momentum in that direction. The localization in position space is thus nicely reflected by the significant enhancements in the directions $(\varphi = \pi/2, 3\pi/2)$ of the orbit.

an upper bound for the counting function $N_{\mathrm{bb}}(E)$ of bouncing ball modes,

$$\lim_{E\to\infty} \frac{N_{\mathrm{bb}}(E)}{N(E)} = 0 \ . \tag{39}$$

Further information on the asymptotic behaviour of the counting function of such localized states is provided in [118], where a heuristic argument shows

$$N_{\mathrm{bb}}(E) \sim \alpha E^{\delta} \quad , \qquad E \to \infty \quad . \tag{40}$$

From eq. (39) it follows that $\delta < 1$. As shown in [118] the exponent δ is determined by the local shape of the curved boundary connected with the

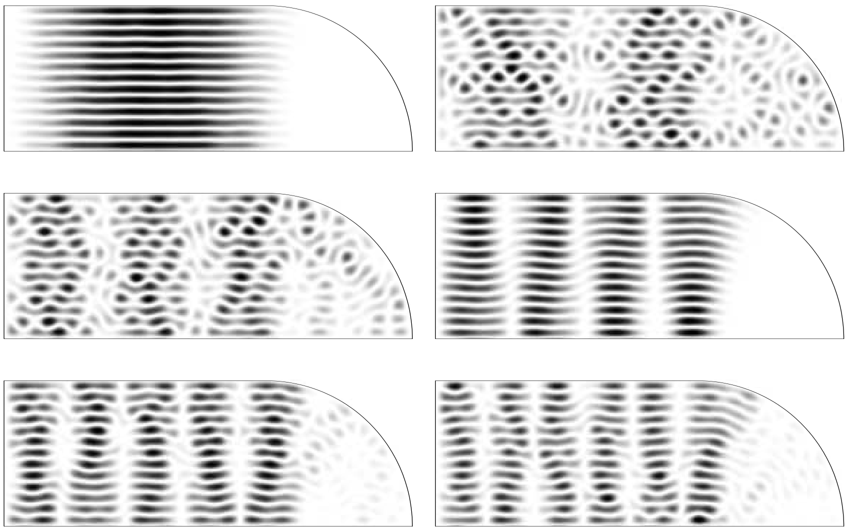

Fig. 14. Density plots of $|\psi_n(\mathbf{q})|^2$ for a consecutive series of bouncing ball modes in the stadium billiard. These eigenfunctions show localization on the rectangular part of the billiard.

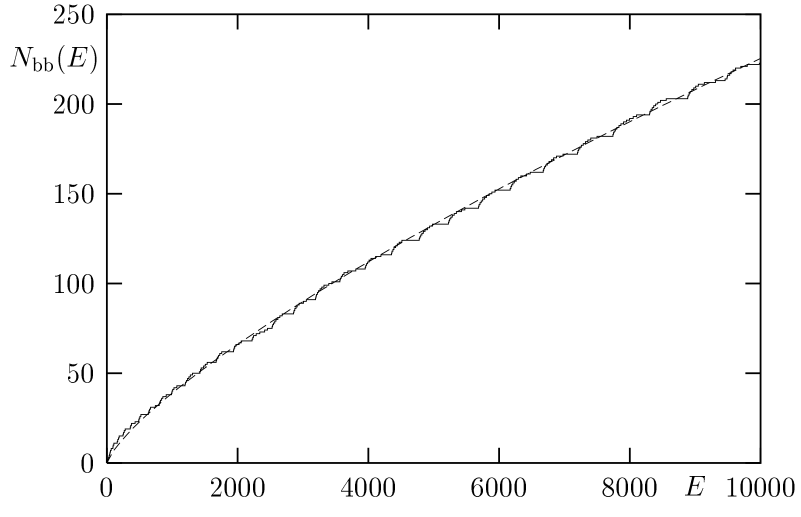

Fig. 15. The number $N_{\mathrm{bb}}(E)$ of bouncing ball modes for the stadium billiard (odd–odd symmetry) together with the fit αE^{δ}, where $\alpha = 0.20$ and $\delta = 0.76$.

straight segment. For the stadium billiard one gets for the exponent $\delta = 3/4$, which was also obtained in [119] by a different approach. For the Sinai billiard on the torus with a circular scatterer one gets $\delta = 9/10$. Fig. 15 shows the numerically determined counting function $N_{\rm bb}(E)$ obtained from visual selection of bouncing ball states from the first 2000 eigenfunctions of odd–odd symmetry of the stadium billiard. The dashed curve shows the result of a fit to αE^δ giving $\alpha = 0.20$ and $\delta = 0.76$ [118].

A particularly interesting application of this result concerns the question whether one can improve the quantum ergodicity theorem by giving a stronger bound on the number of non-quantum-ergodic states. In [118] it is shown explicitly that for any $\delta < 1$, arbitrarily close to 1, one can find an ergodic billiard possessing $N_{\rm bb}(E) \sim \alpha E^\delta$ for the asymptotic behaviour of the number of the non-quantum-ergodic bouncing ball modes. This shows that the quantum ergodicity theorem cannot be improved without further assumptions on the system.

Another important question concerning the quantum ergodicity theorem is the rate by which quantum mechanical expectation values tend to their corresponding limit. This can be studied quantitatively by considering the quantities

$$S_m(E,A) = \frac{1}{N(E)} \sum_{E_n \le E} \left| \langle \psi_n, A\psi_n \rangle - \overline{\sigma(A)} \right|^m \quad . \tag{41}$$

Quantum ergodicity is equivalent to $S_m(E,A) \to 0$ for $E \to \infty$ and $m \ge 1$. Several arguments suggest a rate

$$S_1(E,A) \sim E^{-\frac{1}{4}} \qquad \text{as } E \to \infty \quad , \tag{42}$$

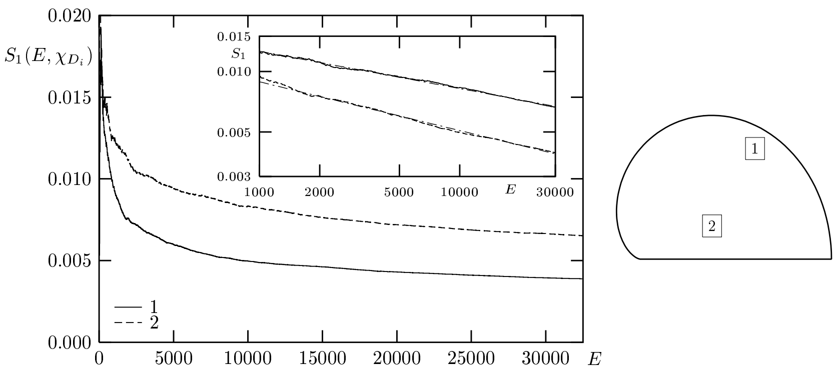

Fig. 16. Rate of quantum ergodicity $S_1(E,A)$ for the cardioid billiard for two observables being the characteristic functions χ_{D_i} of the domains D_1 and D_2 in the desymmetrized cardioid billiard as shown to the right. The inset shows the same curves in a double logarithmic plot together with the result of a fit to $S_1^{\rm fit}(E) = aE^{-1/4+\epsilon}$.

see [104] for a summary on the proven and conjectured behaviour of $S_m(E,A)$. Detailed studies of the rate of quantum ergodicity on surfaces of constant negative curvature and for Euclidean billiards can be found in [71,104].

In fig. 16 the numerically computed rate $S_1(E,A)$ for $A=\chi_{D_i}$ is shown. A fit to $S_1^{\rm fit}(E)=aE^{-1/4+\epsilon}$ gives $\epsilon=0.007$ for $A=\chi_{D_1}$ and $\epsilon=0.064$ for $A=\chi_{D_2}$. Thus in the first case there is very good agreement with the expectation (42), whereas in the second case a significant deviation is observed. This deviation is caused by a considerable number of localized eigenfunctions, like the one in fig. 13, i.e., a subsequence where the quantum limit may be different from the Liouville measure. In [104] it is shown that if the counting function for such a subsequence of localized eigenfunctions increases more strongly than $E^{3/4}$ then the rate of quantum ergodicity is slower than (42). In contrast to Euclidean billiards, for surfaces of constant negative curvature the rate of quantum ergodicity was always found to be in excellent agreement with $E^{-1/4}$ [71].

5 Other topics

In the foregoing sections we have discussed some of our results obtained within the Schwerpunktprogramm (SPP) during the years 1994–1999. We would like to conclude by giving a very short summary of the other results achieved by our group within the same programme. (Here we do not mention our results on topics different from the research projects of the SPP.)

Several papers have been devoted to the study of quantum chaos in three–dimensional systems. In [70] an exact Selberg trace formula has been derived for compact polyhedral billiards which tesselate the three–dimensional hyperbolic space of constant negative curvature. For a tetrahedral billiard being strongly chaotic, part of the length spectrum of periodic orbits and of the energy spectrum has been computed. Recently the tetrahedral billiard has found a fascinating application in cosmology [120] where the evolution of initial metric perturbations of a small hyperbolic universe are computed from the eigenvalues and eigenfunctions of the Laplace–Beltrami operator yielding the angular power spectrum of the fluctuations of the cosmic microwave background. Asymptotic laws for the mean multiplicities of lengths of closed geodesics in arithmetic hyperbolic three–orbifolds have been derived in [69]. The Selberg trace formula, the Selberg zeta function and the cosine quantization rule have been discussed in detail [68] for Picard's billiard which is a non–compact three–dimensional arithmetical billiard defined on the fundamental domain of the Picard group $\mathrm{PSL}(2,\mathbb{Z}[\mathrm{i}])$.

Based on the theory of Hecke operators a numerical algorithm has been worked out and applied [22] to compute a large number of very precise eigenvalues of the Laplacian for several three–dimensional, non–compact billiards in the hyperbolic upper half space defined on the fundamental domains of the groups $\mathrm{PSL}(2,\mathcal{O})$, where $\mathcal{O}$ is the ring of integers of the imaginary quadratic number fields $\mathbb{Q}(\sqrt{-D})$, $D = 1$ (Picard group), 2, 3, 7, 11, 19. These systems provide further examples of arithmetic quantum chaos by possessing spectral statistics close to Poissonian [22].

The paper [121] contains a new derivation of the semiclassical trace formula for billiards in three dimensions starting from a boundary integral equation. A practical method for determining the monodromy matrix and the Maslov index in three dimensions is described.

The chaotic scattering in a two–dimensional Coulombic muffin–tin potential has been studied in [122,123]. Using the thermodynamic formalism the Hausdorff dimension, escape rate and Kolmogorov–Sinai entropy of the system has been determined. Furthermore, the statistics of the scattering phases have been investigated.

In [124] quantization rules based on Selberg's trace formula have been investigated for the geodesic motion on two compact Riemannian surfaces of genus two and on the triangular billiard $T^*(2,3,8)$.

The quantum mechanical time evolution (2) implies that the autocorrelation function

$$C(t) := \langle \Psi(0) | \Psi(t) \rangle = \sum_{n=1}^{\infty} |c_n|^2 \mathrm{e}^{-\frac{\mathrm{i}}{\hbar} E_n t} \tag{43}$$

has the mathematical form of a generalized Weyl sum. If the eigenvalues are at most quadratic in n, i.e., $E_n = an^2 + bn + c$, one obtains under certain conditions on the coefficients $|c_n|^2$ the classical Jacobi theta function. It turns out that $C(t)$ shows as a function of t quite a "chaotic" behaviour in the complex plane. Exploiting ergodic theory, it was possible [125–127] to derive several theorems on the value distribution of certain theta sums which have important applications in quantum mechanics. (See also [128].)

For sytems which are neither chaotic nor integrable but show a complicated mixture of regular and chaotic behaviour, the semiclassical periodic-orbit approximations are more complicated than in the original Gutzwiller trace formula (26). In [129–131] uniform approximations for contributions to Gutzwiller's periodic–orbit sum for the spectral density have been derived which are valid close to bifurcations of periodic orbits in sytems with mixed phase space. Results are given for the tangent, the period–doubling, the period–tripling and for generic period–quadrupling bifurcations. Bifurcations occur also in parameter–dependent integrable systems. As an example, the elliptical billiard and its transition to an oval billiard has been studied in [129]. Uniform approximations for diffractive contributions to the trace formula in billiard systems with corners have been worked out in [132].

In [133,134] semiclassical methods are used to explain the mass asymmetry in nuclear fission and the properties of metal clusters and quantum dots.

Acknowledgments

We would like to thank Dr. R. Aurich, Dr. J. Bolte, Dr. S. Brandis, Prof. N. Chernov, Dr. H. Dullin, Dr. J. Marklof, Dr. C. Matthies, Dr. H. Ninnemann, R. Schubert, Dr. M. Sieber, G. Steil, Dr. P. Stifter and M. Taglieber for the fruitful collaboration in the SPP. We are grateful to Dr. R. Aurich for the kind provision of the numerical results for the mode–fluctuation distribution displayed in fig. 8. Furthermore we would like to thank Prof. M. Robnik and Dr. T. Prosen for the kind provision of the eigenvalues of the cardioid billiard. Fig. 13 is visualized using `Geomview` from *The Geometry Center* of the University of Minnesota and then rendered using `Blue Moon Rendering Tools` written by L.I. Gritz. Financial support by the Deutsche Forschungsgemeinschaft DFG is gratefully acknowledged.

References

1. R. Aurich and F. Steiner: *Temporal quantum chaos*, Int. J. Mod. Phys. B **13** (1999) 2361-2369.
2. M. C. Gutzwiller: *Chaos in Classical and Quantum Mechanics*, Springer-Verlag, New York, (1990).
3. M. V. Berry and M. Tabor: *Level clustering in the regular spectrum*, Proc. R. Soc. London Ser. A **356** (1977) 375–394.
4. O. Bohigas, M.-J. Giannoni and C. Schmit: *Characterization of chaotic quantum spectra and universality of level fluctuation laws*, Phys. Rev. Lett. **52** (1984) 1–4.
5. M. L. Mehta: *Random Matrices*, Academic Press, San Diego, revised and enlarged second edn., (1991).
6. A. Bäcker, F. Steiner and P. Stifter: *Spectral statistics in the quantized cardioid billiard*, Phys. Rev. E **52** (1995) 2463–2472.
7. R. Aurich, A. Bäcker and F. Steiner: *Mode fluctuations as fingerprints of chaotic and non-chaotic systems*, Int. J. Mod. Phys. B **11** (1997) 805–849.
8. H. P. Baltes and E. R. Hilf: *Spectra of Finite Systems*, Bibliographisches Institut, Mannheim, Wien, Zürich, (1976).
9. M. Berry: *Semiclassical formula for the number variance of the Riemann zeros*, Nonlinearity **1** (1988) 399–407.
10. R. Aurich and F. Steiner: *Energy-level statistics of the Hadamard-Gutzwiller ensemble*, Physica D **43** (1990) 155–180.
11. A. Cheng and J. L. Lebowitz: *Statistics of energy levels in integrable quantum systems*, Phys. Rev. A **44** (1991) R3399–R3401.
12. R. Aurich and F. Steiner: *Periodic–orbit theory of the number variance $\Sigma^2(L)$ of strongly chaotic systems*, Physica D **82** (1995) 266–287.
13. R. Aurich, F. Scheffler and F. Steiner: *On the subtleties of arithmetical quantum chaos*, Phys. Rev. E **51** (1995) 4173–4189.
14. P. M. Bleher and J. L. Lebowitz: *Variance of number of lattice points in random narrow elliptic strip*, Ann. Inst. Henri Poincaré: Probab. et Statist. **31** (1995) 27–58.
15. M. V. Berry: *Semiclassical theory of spectral rigidity*, Proc. R. Soc. London Ser. A **400** (1985) 229–251.
16. R. Aurich and F. Steiner: *On the periodic orbits of a strongly chaotic system*, Physica D **32** (1988) 451–460.

17. R. Aurich, E. B. Bogomolny and F. Steiner: *Periodic orbits on the regular hyperbolic octagon*, Physica D **48** (1991) 91–101.
18. E. B. Bogomolny, B. Georgeot, M.-J. Giannoni and C. Schmit: *Chaotic billiards generated by arithmetic groups*, Phys. Rev. Lett. **69** (1992) 1477–1480.
19. J. Bolte, G. Steil and F. Steiner: *Arithmetical chaos and violation of universality in energy level statistics*, Phys. Rev. Lett. **69** (1992) 2188–2191.
20. J. Bolte: *Some studies on arithmetical chaos in classical and quantum mechanics*, Int. J. Mod. Phys B **7** (1993) 4451–4553.
21. P. Sarnak: *Arithmetic quantum chaos*, Israel Math. Conf. Proc. **8** (1995) 183–236.
22. G. Steil: *Eigenvalues of the Laplacian for Bianchi groups*, in: *Emerging Applications of Number Theory* [135], pp. 617–641.
23. J. P. Keating: *The cat maps: Quantum mechanics and classical motion*, Nonlinearity **4** (1991) 309–341,
24. P. Sarnak: *Values at integers of binary quadratic forms*, in: *Harmonic analysis and number theory* (Montreal 1996), CMS Conf. Proc. **21**, American Mathematical Society, Providence, RI (1997) 181–203.
25. A. Eskin, G. A. Margulis and S. Mozes: *Quadratic forms of signature (2,2) and eigenvalue spacings on rectangular 2-tori*, preprint, `http://zaphod.uchicago.edu/~eskin/` (1998).
26. A. Pandey, O. Bohigas and M.-J. Giannoni: *Level repulsion in the spectrum of two–dimensional harmonic oscillators*, J. Phys. A **22** (1989) 4083–4088.
27. P. M. Bleher: *The energy level spacing for two harmonic oscillators with golden mean ratio of frequencies*, J. Statist. Phys. **61** (1990) 869–876.
28. P. M. Bleher: *The energy level spacing for two harmonic oscillators with generic ratio of frequencies*, J. Statist. Phys. **63** (1991) 261–283.
29. C. D. Greenman: *The generic spacing distribution of the two-dimensional harmonic oscillator*, J. Phys. A **29** (1996) 4065–4081.
30. J. Marklof: *The n-point correlations between values of a linear form*, preprint IHES/M/98/66, with an appendix *The number of solutions of simultaneous quadratic equations* by Z. Rudnick (1998). To appear in Ergodic Theory Dynam. Systems.
31. A. Bouzouina and S.-D. Bièvre: *Equipartition of the eigenfunctions of quantized ergodic maps on the torus*, Commun. Math. Phys. **178** (1996) 83–105.
32. S. De Bièvre, M. Degli Esposti and R. Giachetti: *Quantization of a class of piecewise affine transformations on the torus.*, Commun. Math. Phys. **176** (1996) 73–94.
33. J. Marklof and Z. Rudnick: *Quantum unique ergodicity for parabolic maps*, preprint IHES/M/99/01, math-ph/9901001 (1999). To appear in Geometric and Functional Analysis.
34. A. Bäcker and G. Haag: *Spectral statistics for quantized skew translations on the torus,*, J. Phys. A **32** (1999) L393-L398.
35. F. Steiner: *Quantum chaos*, in *Schlaglichter der Forschung. Zum 75. Jahrestag der Universität Hamburg 1994*, (ed. R. Ansorge) Festschrift published on the occasion of the 75th anniversary of the University of Hamburg, pp. 543–564, Dietrich Reimer Verlag, Berlin und Hamburg (1994).
36. R. Aurich, J. Bolte and F. Steiner: *Universal signatures of quantum chaos*, Phys. Rev. Lett. **73** (1994) 1356–1359.

37. J. Bolte: *Semiclassical trace formulae and eigenvalue statistics in quantum chaos*, Open Syst. Inf. Dynamics **6** (1999) 167–226.
38. A. Selberg: *Contributions to the theory of the Riemann zeta-function*, Arch. Math. Naturvid. **48** (1946) 89–155.
39. H. L. Montgomery: *Selberg's work on the zeta-function*, in: *Number theory, trace formulas and discrete groups (Symposium in Honor of Atle Selberg, Oslo, July 14-21, 1987)* (Eds. K. E. Aubert, E. Bombieri and D. Goldfeld), pp. 157–168, Academic Press, (1989).
40. A. Selberg: *Collected Papers, Vol. II*, Springer-Verlag, Heidelberg, (1991).
41. P. M. Bleher, F. J. Dyson and J. L. Lebowitz: *Non–Gaussian energy level statistics for some integrable systems*, Phys. Rev. Lett. **71** (1993) 3047–3050.
42. P. M. Bleher: *Trace formula for quantum integrable systems, lattice-point problem, and small divisors*, in: *Emerging Applications of Number Theory* [135], pp. 1–38.
43. A. S. Besicovitch: *Almost Periodic Functions*, Dover Pub., Cambridge, (1954).
44. P. M. Bleher: *On the distribution of the number of lattice points inside a family of convex ovals*, Duke Math. J. **67** (1992) 461–481.
45. G. H. Hardy: *The average order of the arithmetical functions $P(x)$ and $\Delta(x)$*, Proc. London Math. Soc. **15** (1915) 192–213.
46. M. N. Huxley: *Exponential sums and lattice points*, Proc. London Math. Soc. **66** (1993) 279–301.
47. D. R. Heath-Brown: *The distribution and moments of the error term in the Dirichlet divisor problem*, Acta Arithmetica **60** (1992) 389–415.
48. R. Aurich: private communication.
49. A. M. Odlyzko: private communication.
50. H. Alt, A. Bäcker, C. Dembowski, H.-D. Gräf, R. Hofferbert, H. Rehfeld and A. Richter: *Mode fluctuation distribution for spectra of superconducting microwave billiards*, Phys. Rev. E **58** (1998) 1737–1742.
51. R. Schubert: *The trace formula and the distribution of eigenvalues of Schrödinger operators on manifolds all of whose geodesics are closed*, DESY report, DESY 95–090.
52. M. C. Gutzwiller: *Periodic orbits and classical quantization conditions*, J. Math. Phys. **12** (1971) 343–358.
53. M. Sieber and F. Steiner: *Classical and quantum mechanics of a strongly chaotic billiard system*, Physica D **44** (1990) 248–266.
54. M. Sieber and F. Steiner: *Generalized periodic-orbit sum rules for strongly chaotic systems*, Phys. Lett. A **144** (1990) 159–163.
55. Y. Colin de Verdière: *Spectre du laplacien et longueurs des géodésiques périodiques I* (in French), Compositio Math. **27** (1973) 83–106.
56. Y. Colin de Verdière: *Spectre du laplacien et longueurs des géodésiques périodiques II* (in French), Compositio Math. **27** (1973) 159–184.
57. J. Chazarain: *Formule de Poisson pour les variétés Riemanniennes* (in French), Invent. Math. **24** (1974) 65–82.
58. J. J. Duistermaat and V. W. Guillemin: *The spectrum of positive elliptic operators and periodic bicharacteristics*, Invent. Math. **29** (1975) 39–79.
59. V. Guillemin and A. Uribe: *Reduction and the trace formula*, J. Differ. Geom. **32** (1990) 315–347.
60. R. Brummelhuis and A. Uribe: *A semi-classical trace formula for Schrödinger operators*, Commun. Math. Phys. **136** (1991) 567–584.

61. T. Paul and A. Uribe: *Sur la formule semi-classique des traces* (in French), C. R. Acad. Sci., Paris, Ser. I **313** (1991) 217–222.
62. E. Meinrenken: *Semiclassical principal symbols and Gutzwiller's trace formula*, Rep. Math. Phys. **31** (1992) 279–295.
63. R. Aurich, M. Sieber and F. Steiner: *Quantum chaos of the Hadamard-Gutzwiller model*, Phys. Rev. Lett. **61** (1988) 483–487.
64. R. Aurich and F. Steiner: *Periodic-orbit sum rules for the Hadamard-Gutzwiller model*, Physica D **39** (1989) 169–193.
65. R. Aurich and F. Steiner: *From classical periodic orbits to the quantization of chaos*, Proc. R. Soc. London Ser. A **437** (1992) 693–714.
66. R. Aurich and F. Steiner: *Staircase functions, spectral rigidity and a rule for quantizing chaos*, Phys. Rev. A **45** (1992) 583–592.
67. R. Aurich and F. Steiner: *Statistical properties of highly excited quantum eigenstates of a strongly chaotic system*, Physica D **64** (1993) 185–214.
68. C. Matthies: *Picards Billard. Ein Modell für Arithmetisches Quantenchaos in drei Dimensionen*, Ph.D. thesis, II. Institut für Theoretische Physik, Universität Hamburg, (1995).
69. J. Marklof: *On multiplicities in length spectra of arithmetic hyperbolic three-orbifolds*, Nonlinearity **9** (1996) 517–536.
70. R. Aurich and J. Marklof: *Trace formulae for three-dimensional hyperbolic lattices and application to a strongly chaotic tetrahedral billiard*, Physica D **92** (1996) 101–129.
71. R. Aurich and M. Taglieber: *On the rate of quantum ergodicity on hyperbolic surfaces and for billiards*, Physica D **118** (1998) 84–102.
72. M. Sieber and F. Steiner: *Quantum chaos in the hyperbola billiard*, Phys. Lett. A **148** (1990) 415–419.
73. M. Abramowitz and I. A. Stegun (eds.): *Pocketbook of Mathematical Functions*, Verlag Harri Deutsch, Thun – Frankfurt/Main, abridged edn., (1984).
74. R. Aurich, C. Matthies, M. Sieber and F. Steiner: *Novel rule for quantizing chaos*, Phys. Rev. Lett. **68** (1992) 1629–1632.
75. A. Bäcker: *Classical and Quantum Chaos in Billiards*, Ph.D. thesis, Abteilung Theoretische Physik, Universität Ulm, (1998).
76. L. A. Bunimovich and Ya. G. Sinai: *Markov partitions for dispersed billiards*, Commun. Math. Phys. **78** (1980) 247–280, erratum, ibid. **107** (1986) 357–358.
77. L. A. Bunimovich, Ya. G. Sinai and N. I. Chernov: *Markov partitions for two-dimensional hyperbolic billiards*, Russ. Math. Surveys **45** (1990) 105–152.
78. T. Krüger and S. Troubetzkoy: *Markov partitions and shadowing for non-uniformly hyperbolic systems with singularities*, Ergodic Theory Dynam. Systems **12** (1992) 487–508.
79. T. Krüger and S. Troubetzkoy: *Symbolic dynamics via shadowing for diffeomorphisms with non zero exponents*, preprint (1997).
80. V. M. Alekseev and M. V. Yakobson: *Symbolic dynamics and hyperbolic dynamic systems*, Physics Reports **75** (1981) 287–325.
81. A. Bäcker and N. Chernov: *Generating partitions for two-dimensional hyperbolic maps*, Nonlinearity **11** (1998) 79–87.
82. O. Biham and M. Kvale: *Unstable periodic orbits in the stadium billiard*, Phys. Rev. A **46** (1992) 6334–6339.
83. H. Bruus and N. D. Whelan: *Edge diffraction, trace formulae and the cardioid billiard*, Nonlinearity **9** (1996) 1023–1047.

84. A. Bäcker and H. R. Dullin: *Symbolic dynamics and periodic orbits for the cardioid billiard*, J. Phys. A **30** (1997) 1991–2020.
85. P. Cvitanović, G. Gunaratne and I. Procaccia: *Topological and metric properties of Hénon-type strange attractors*, Phys. Rev. A **38** (1988) 1503–1520.
86. A. de Carvalho: *Pruning fronts and the formation of horseshoes*, Ergodic Theory Dynam. Systems **19** (1999) 851–894.
87. Y. Ishii: *Towards the kneading theory for Lozi mappings I: A solution of the pruning front conjecture and the first tangency problem*, Nonlinearity **10** (1997) 731–747.
88. E. P. Wigner: *On the quantum correction for thermodynamic equilibrium*, Phys. Rev. **40** (1932) 749–759.
89. M. V. Berry: *Regular and irregular semiclassical wavefunctions*, J. Phys. A **10** (1977) 2083–2091.
90. A. Voros: *Semi-classical ergodicity of quantum eigenstates in the Wigner representation*, in: *Stochastic Behavior in Classical and Quantum Hamiltonian Systems*, no. 93 in Lecture Notes in Physics, 326–333, Springer-Verlag, Berlin, (1979).
91. M. V. Berry: *Semiclassical mechanics of regular and irregular motion*, in: *Comportement Chaotique des Systèmes Déterministes — Chaotic Behaviour of Deterministic Systems* (Eds. G. Iooss, R. H. G. Hellemann and R. Stora), 171–271, North-Holland, Amsterdam, (1983).
92. V. I. Arnold: *Modes and quasimodes*, Funct. Anal. Appl. **6** (1972) 94–101.
93. V. F. Lazutkin: *Asymptotics of the eigenvalues of the Laplacian and quasimodes. A series of quasimodes corresponding to a system of caustics close to the boundary*, Math. USSR Izv. **7** (1973) 439–466.
94. Y. Colin de Verdière: *Quasi-modes sur les variétés Riemanniennes* (in French), Invent. Math. **43** (1977) 15–52.
95. V. F. Lazutkin: *KAM theory and semiclassical approximations to eigenfunctions*, Springer-Verlag, Berlin, (1993).
96. A. I. Shnirelman: *Ergodic properties of eigenfunctions* (in Russian), Usp. Math. Nauk **29** (1974) 181–182.
97. A. I. Shnirelman: *On the asymptotic properties of eigenfunctions in the regions of chaotic motion*, in: V. F. Lazutkin: *KAM Theory and Semiclassical Approximations to Eigenfunctions*, Springer-Verlag Berlin (1993).
98. S. Zelditch: *Uniform distribution of eigenfunctions on compact hyperbolic surfaces*, Duke. Math. J. **55** (1987) 919–941.
99. Y. Colin de Verdière: *Ergodicité et fonctions propres du laplacien* (in French), Commun. Math. Phys. **102** (1985) 497–502.
100. B. Helffer, A. Martinez and D. Robert: *Ergodicité et limite semi-classique* (in French), Commun. Math. Phys. **109** (1987) 313–326.
101. P. Gérard and E. Leichtnam: *Ergodic properties of eigenfunctions for the Dirichlet problem*, Duke Math. J. **71** (1993) 559–607.
102. S. Zelditch and M. Zworski: *Ergodicity of eigenfunctions for ergodic billiards*, Commun. Math. Phys. **175** (1996) 673–682.
103. A. Knauf and Ya. G. Sinai (with a contribution by V. Baladi): *Classical Nonintegrability, Quantum Chaos*, DMV–Seminar 27, Birkhäuser, Basel, (1997).
104. A. Bäcker, R. Schubert and P. Stifter: *Rate of quantum ergodicity in Euclidean billiards*, Phys. Rev. E **57** (1998) 5425–5447, erratum ibid. **58** (1998) 5192.

105. L. Hörmander: *The Analysis of Linear Partial Differential Operators III*, Springer-Verlag, Berlin, Heidelberg, (1985).
106. G. B. Folland: *Harmonic Analysis in Phase Space*, vol. 122 of *Annals of Mathematics Studies*, Princeton University Press, Princeton, (1989).
107. M. E. Taylor: *Pseudodifferential Operators*, no. 34 in Princeton Mathematical Series, Princeton University Press, Princeton, New Jersey, (1981).
108. R. Schubert: *Mikrolokale Analysis und Spurformeln*, (1996), Diploma thesis, II. Institut für Theoretische Physik, Universität Hamburg.
109. M. Degli Esposti, S. Graffi and S. Isola: *Classical limit of the quantized hyperbolic toral automorphisms*, Commun. Math. Phys. **167** (1995) 471–507.
110. S. De Bièvre and M. Degli Esposti: *Egorov theorems and equidistribution of eigenfunctions for the quantized sawtooth and baker maps*, Ann. Inst. Henri Poincaré, Physique Théorique **69** (1996) 1–30.
111. A. Bäcker and R. Schubert: *Chaotic eigenfunctions in momentum space*, J. Phys. A **32** (1999) 4795–4815.
112. Z. Rudnick and P. Sarnak: *The behaviour of eigenstates of arithmetic hyperbolic manifolds*, Commun. Math. Phys. **161** (1994) 195–213.
113. R. Aurich and F. Steiner: *Quantum eigenstates of a strongly chaotic system and the scar phenomenon*, Chaos, Solitons and Fractals **5** (1995) 229–255.
114. O. M. Auslaender and S. Fishman: *Exact eigenfunctions of a chaotic system*, Physica D **128** (1999) 180–223.
115. E. J. Heller: *Bound-state eigenfunctions of classically chaotic Hamiltonian systems: Scars of periodic orbits*, Phys. Rev. Lett. **53** (1984) 1515–1518.
116. S. W. McDonald and A. N. Kaufmann: *Wave chaos in the stadium: Statistical properties of short-wave solutions of the Helmholtz equation*, Phys. Rev. A **37** (1988) 3067–3086.
117. R. Aurich, A. Bäcker, R. Schubert and M. Taglieber: *Maximum norms of chaotic quantum eigenstates and random waves*, Physica D **129** (1999) 1–14.
118. A. Bäcker, R. Schubert and P. Stifter: *On the number of bouncing-ball modes in billiards*, J. Phys. A **30** (1997) 6783–6795.
119. G. Tanner: *How chaotic is the stadium billiard? A semiclassical analysis*, J. Phys. A **30** (1997) 2863–2888.
120. R. Aurich: *The fluctuations of the cosmic microwave background for a compact hyperbolic universe*, Astrophys. J. **524** (1999) 497-503.
121. M. Sieber: *Billiard systems in three dimensions: the boundary integral equation and the trace formula*, Nonlinearity **11** (1998) 1607–1623.
122. S. Brandis: *Chaos in a Coulombic muffin-tin potential*, Phys. Rev. E **51** (1995) 3023–3031.
123. S. Brandis: *Classical and Quantum Chaotic Scattering in a Muffin–Tin Potential*, Ph.D. thesis, II. Institut für Theoretische Physik, Universität Hamburg, (1995), DESY report DESY 95–101.
124. H. Ninnemann: *Gutzwiller's octagon and the triangular billiard $T^*(2,3,8)$ as models for the quantization of chaotic systems by Selberg's trace formula*, Int. J. Mod. Phys B **9** (1995) 1647–1753.
125. J. Marklof: *Limit theorems for theta sums*, Duke Mathematical Journal **97** (1999) 127–153.
126. J. Marklof: *Limit Theorems for Theta Sums with Applications in Quantum Mechanics*, Shaker Verlag, Aachen, (1997), Dissertation, Universität Ulm, 1997.

127. J. Marklof: *Theta sums, Eisenstein series, and the semiclassical dynamics of a precessing spin*, in: *Emerging Applications of Number Theory* [135], pp. 405–450.
128. P. Stifter, C. Leichtle, W. P. Schleich and J. Marklof: *Das Teilchen im Kasten: Strukturen in der Wahrscheinlichkeitsdichte*, Zeitschrift für Naturforschung **52a** (1997) 377–385.
129. M. Sieber: *Semiclassical transition from an elliptical to an oval billiard*, J. Phys. A **30** (1997) 4563–4596.
130. H. Schomerus and M. Sieber: *Bifurcations of periodic orbits and uniform approximations*, J. Phys. A **30** (1997) 4537–4562.
131. M. Sieber and H. Schomerus: *Uniform approximation for period-quadrupling bifurcations*, J. Phys. A **31** (1998) 165–183.
132. M. Sieber, N. Pavloff and C. Schmit: *Uniform approximation for diffractive contributions to the trace formula in billiard systems*, Phys. Rev. E **55** (1997) 2279–2299.
133. M. Brack, S. M. Reimann and M. Sieber: *Semiclassical interpretation of the mass asymmetry in nuclear fission*, Phys. Rev. Lett. **79** (1997) 1817–1820.
134. M. Brack, P. Meier, S. M. Reimann and M. Sieber: *Manifestation of classical orbits in nuclei, metal clusters and quantum dots*, in: *Proceedings of the International Symposium on Similarities and Differences between Atomic Nuclei and Microclusters, Tsukuba, July 1-4, 1997* (Eds. Y. Abe, I. Arai, S. M. Lee and K. Yabana), pp. 17–28. American Institute of Physics, (1998).
135. D. A. Hejhal, J. Friedman, M. C. Gutzwiller and A. M. Odlyzko (eds.): *Emerging Applications of Number Theory*, The IMA Volumes in Mathematics and its Applications, Vol. **109**, Springer-Verlag, (1999).